

Modelling and Simulation of Scramjet Engine

a project presented to
The Faculty of the Department of Aerospace Engineering
San José State University

in partial fulfillment of the requirements for the degree
Master of Science in Aerospace Engineering

by

Naga Ravi Teja Palnati

December 2018

approved by

Dr. Periklis Papadopoulos
Faculty Advisor



Contents

Modelling and Simulation of Scramjet Combustion Chamber.....	6
1. Introduction	6
1.1 Theory	6
1.2 History	7
1.3 Mesh and mesh refinement	10
1.4 Grid independence study.....	12
2. Results and Discussion	13
2.1 Results	13
2.2 Comparison of Results	18
2.3 Conclusion.....	34
Modelling and Simulation of Scramjet Engine with different Inlets.....	36
1. Introduction	36
1.1 Theory	36
1.2 Boundary conditions.....	38
1.3 Numerical Modelling.....	38
2. Results and Discussion	41
2.1 Results	41
2.2 Conclusion.....	46
References.....	47
Appendix	48

List of Figures

Figure 1: Scramjet engine model	6
Figure 2: NASA X-43 A model	7
Figure 3: Geometry of a) Standard DLR scramjet, b) Spherical cavity and c) Step cavity Combustion chamber	9
Figure 4: Mesh sizing.....	11
Figure 5: Mesh elements.....	11
Figure 6: Grid independence study.....	12
Figure 7: Pressure Contours of a) Standard DLR scramjet, b) Spherical cavity and c) Step cavity	14
Figure 8: Density Contours of a) Standard DLR scramjet, b) Spherical cavity and c) Step cavity.....	15
Figure 9: Velocity Contours of a) Standard DLR scramjet, b) Spherical cavity and c) Step cavity	16
Figure 10: Temperature Contours of a) Standard DLR scramjet, b) Spherical cavity and c) Step cavity	17
Figure 11: Pressure contours of spherical cavity Scramjet Combustion chamber with a) Regular Mesh and b) Refined mesh	18
Figure 12: Density contours of spherical cavity Scramjet Combustion chamber with a) Regular Mesh and b) Refined mesh	19
Figure 13: Temperature contours of spherical cavity Scramjet Combustion chamber with a) Regular Mesh and b) Refined mesh	20
Figure 14: Velocity contours of spherical cavity Scramjet Combustion chamber with a) Regular Mesh and b) Refined mesh	21
Figure 15: Pressure, Velocity, density and Temperature profiles along the length of the combustion chamber	25
Figure 16: Pressure, Density, Velocity and Temperature profiles cross stream of the combustion chamber	31
Figure 17: Pressure variation along the length of the combustion chamber at $y=0\text{mm}$ with a) Regular mesh and b) Refined mesh	33
Figure 18: Pressure variation along the length of the combustion chamber at $y=25\text{mm}$ with a) Regular mesh and b) Refined mesh	34
Figure 19: Flow stations in a Scramjet engine.....	36
Figure 20: Different types of scramjet inlets a) External compression, b) External and internal compression and c) Internal compression	37
Figure 21: Scramjet engine reference model.....	38
Figure 22: External inlet pressure contour at $M=6$	41
Figure 23: External inlet pressure contour at $M=8$	41
Figure 24: External inlet pressure contour at $M=10$	42
Figure 25: External inlet pressure contour at $M=12$	42
Figure 26: Internal and External inlet pressure contour at $M=6$	43
Figure 27: Internal and External inlet pressure contour at $M=8$	43
Figure 28: Internal and External inlet pressure contour at $M=10$	43
Figure 29: Internal and External inlet pressure contour at $M=12$	44
Figure 30: Internal inlet pressure contour at $M=6$	44
Figure 31: Internal inlet pressure contour at $M=8$	45
Figure 32: Internal inlet pressure contour at $M=10$	45
Figure 33: Internal inlet pressure contour at $M=12$	45

Figure 34: External inlet velocity contour at M=6.....	48
Figure 35: External inlet velocity contour at M=8.....	48
Figure 36: External inlet velocity contour at M=10	48
Figure 37: External inlet velocity contour at M=12	49
Figure 38: Internal and external inlet velocity contour at M=6.....	49
Figure 39: Internal and external inlet velocity contour at M=8.....	49
Figure 40: Internal and external inlet velocity contour at M=10.....	50
Figure 41: Internal and external inlet velocity contour at M=12.....	50
Figure 42: Internal inlet velocity contour at M=6	50
Figure 43: Internal inlet velocity contour at M=8	51
Figure 44: Internal inlet velocity contour at M=10	51
Figure 45: Internal inlet velocity contour at M=12	51

List of Tables

Table 1: Boundary conditions	9
------------------------------	---

Modelling and Simulation of Scramjet Combustion Chamber

1. Introduction

1.1 Theory

The Supersonic Combustion Ramjet engine popularly known as Scramjet engine is one of the most promising air breathing engines in the recent times for hypersonic flights where Mach numbers more than 5. Soon, scramjet can fulfill the need of reusable launch vehicles for the space launches and by implementing the scram jet engines, time travel to reach the destinations will be decreased for the civil aviation. The major difference between the regular turbojet engine and the scramjet engine is a compressor. Scramjet engine does not carry the compressor like turbojet engine. So, work of the compressor will be done by the high-speed air and the converging inlet. This decreases the weight of the engine since it does not have moving parts(compressor).

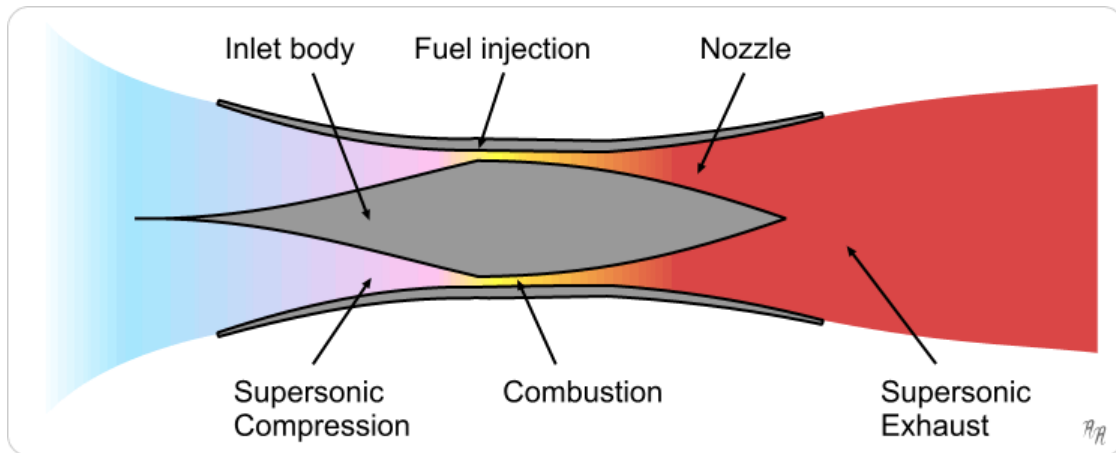


Figure 1: Scramjet engine model

Figure 1 shows a typical scramjet engine. It has a supersonic inlet where the supersonic air enters, and it is compressed; a supersonic combustion chamber, where the compressed air from the inlet is going to be mixed with the fuel; and a diverging nozzle,

where the gases from the combustion chamber accelerated into atmospheric air. NASA has successfully tested the scramjet engine at mach number 5 and ISRO has also successfully tested at mach number 6. Figure 2 shows the NASA Scramjet.



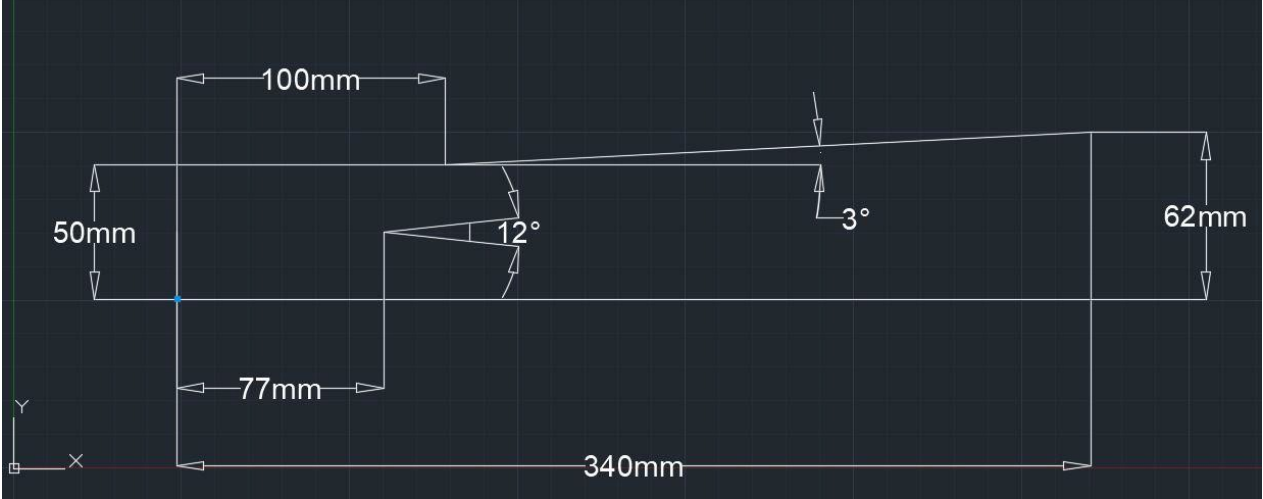
Figure 2: NASA X-43 A model

Along with the advantageous, there are some limitations in scramjet technology. Major drawbacks in the scramjet technology are mixing of high-speed air and fuel and the stabilized combustion. These drawbacks can be overcome by introducing new fuel injection techniques and selecting a fuel which has highest lower heating value. From the previous researches, it was found that hydrogen would be the most preferable fuel for scramjet technology. Cavity based fuel injection techniques will be introduced to achieve stabilized combustion and most efficient high-speed mixing.

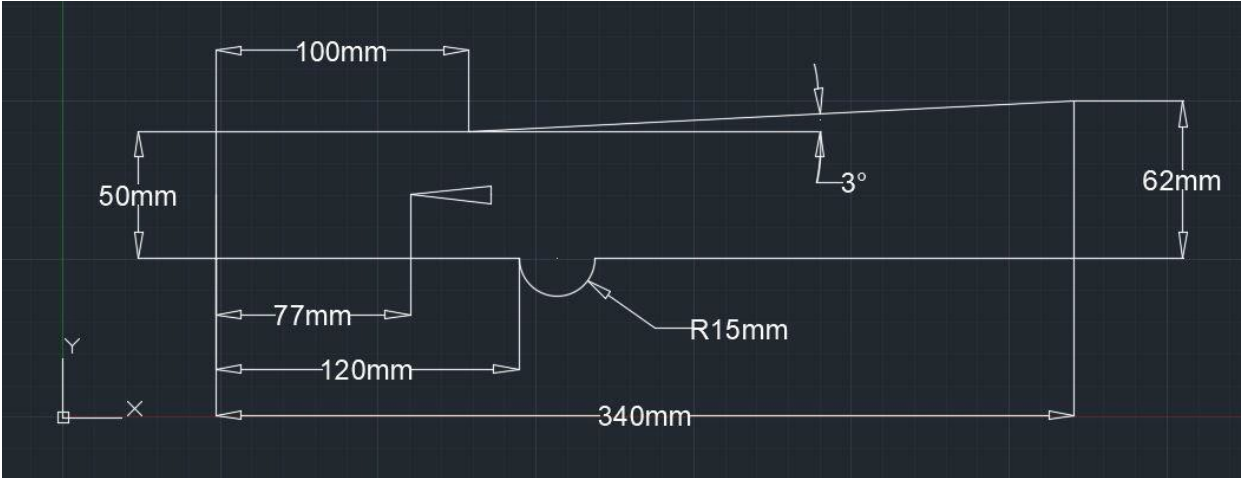
1.2 History

In the previous report, flow simulations of scram jet combustion chamber with different flame holding mechanisms such as step cavity and spherical cavity have been done using the RANS equations, finite eddy dissipation models and SST $k-\omega$ model. Figure 3 shows the CAD diagrams of the models with dimensions. The total length of the combustion chamber is 340mm and height at the inlet is 50mm and at the outlet 62mm. To increase

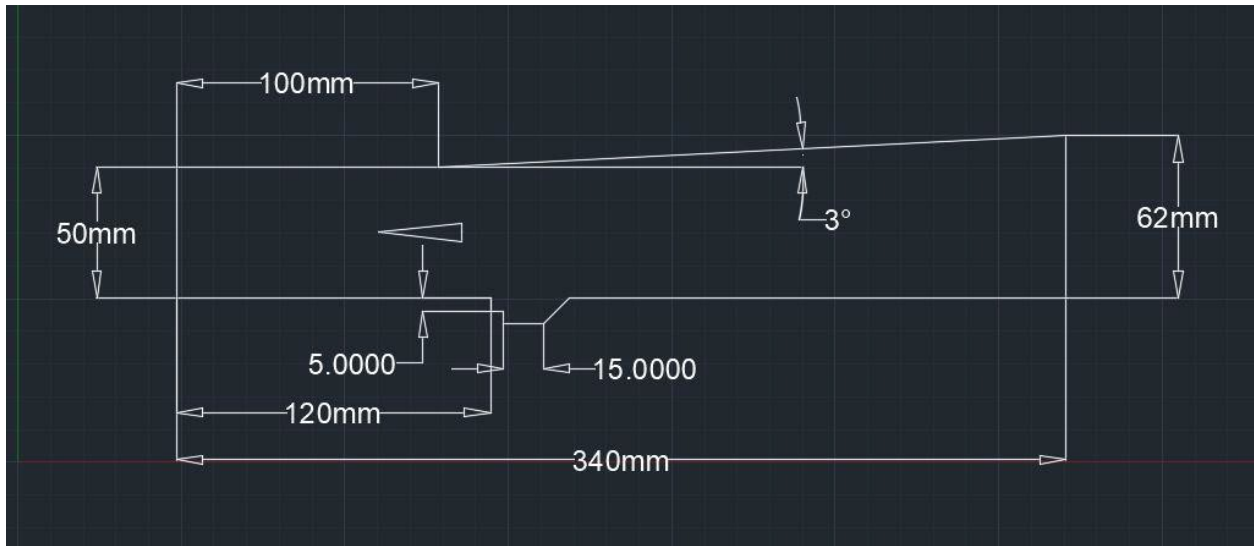
the oblique shock formation, cavity flame holders are placed at 120mm on the lower wall of the combustion chamber.



a)



b)



c)

Figure 3: Geometry of a) Standard DLR scramjet, b) Spherical cavity and c) Step cavity Combustion chamber

The flow simulations of scramjet combustion chamber with step and spherical cavities has been performed using RANS equations, SST $k-\omega$ and finite rate eddy dissipation model. Dirichlet boundary conditions were used for the inlet flow and Neumann boundary conditions were used for the outlet. The assumptions taken into consideration for this project are no slip at the walls of the combustion chamber and computation was performed at steady state. Table 1 shows the boundary conditions considered for the simulation. Meshing has been done with the minimum face size of 0.3mm with fine mesh.

Table 1: Boundary conditions

	Air	Hydrogen
Mach	2	1
u(m/s)	730	1200
T(k)	340	250
P(Pascal)	100000	100000
ρ (kg/m ³)	1.002	0.097

Y_{O_2}	0.232	0
Y_{N_2}	0.736	0
Y_{H_2O}	0.032	0
Y_{H_2}	0	1

From the researches, it was found that the residence time of compressed air in the combustion chamber plays a crucial role in combustion efficiency. From Part A, it was found that cavity-based combustion models generate a good number of shock waves, recirculation zones and vortices which can hold the air for some extra time in the combustion chamber. As a result of that, there will be enough time to mix the fuel with the supersonic air. This increases combustion efficiency. The Contours such as pressure, temperature, velocity and density also have been presented. For the present project, the mesh is going to be refined with a good number of node points than the previous mesh to get the accurate result and these results are going to compare with the previous results.

1.3 Mesh and mesh refinement

The basic idea of meshing is to split the component into a finite number of elements. The accuracy of the meshing depends on the density of the mesh i.e. density is inversely proportional to the accuracy.

Sizing	
Size Function	Curvature
Relevance Center	Fine
<input type="checkbox"/> Max Face Size	0.30 mm
Mesh Defeaturing	Yes
<input type="checkbox"/> Defeature Size	Default (1.5e-003 mm)
<input type="checkbox"/> Growth Rate	Default (1.20)
Span Angle Center	Fine
<input type="checkbox"/> Min Size	5.e-002 mm
<input type="checkbox"/> Curvature Nor...	Default (36.0 °)
Bounding Box Di...	348.610 mm
Minimum Edge L...	6.72670 mm

Figure 4: Mesh sizing

To get the more accurate result, mesh refinement should be done. Simply, mesh refinement is a process of making the mesh elements finer and finer. The convergence of the solution can be judged by the comparison of residual plots. There are two kinds of mesh, one is structured mesh and the second is unstructured mesh. For the present problem, a structural fine mesh is going to be used. The elements presented in the mesh before the mesh refinement was around 55000 and the elements presented in the mesh after refinement is around 210000 which means that the solution after the refinement is almost 4 times accurate.

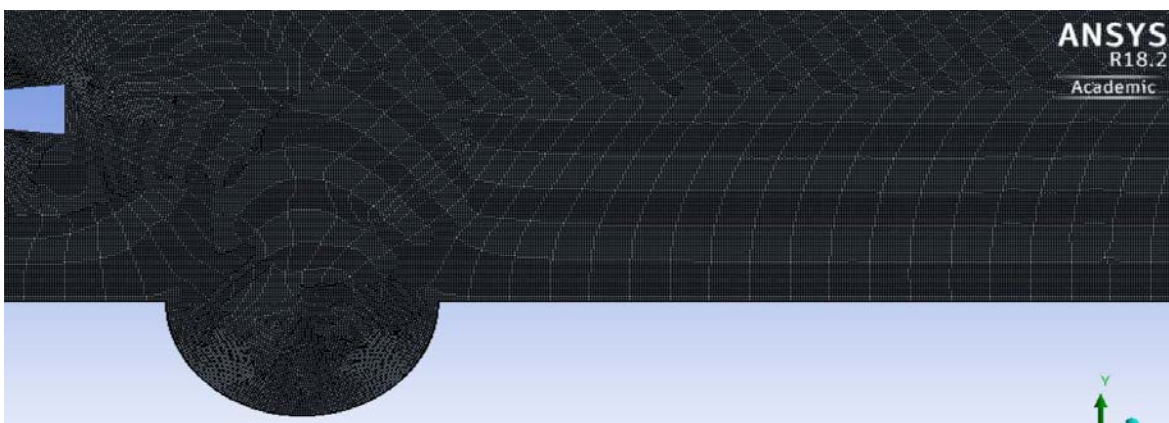


Figure 5: Mesh elements

1.4 Grid independence study

As per the definition of grid independence, if the solution is dependent on the mesh elements or nodes, then the solution is not accurate. So, to get to know the solution is independent of the meshing parameters, grid independence study has been performed. It was found that the solution is independent of the meshing parameters.

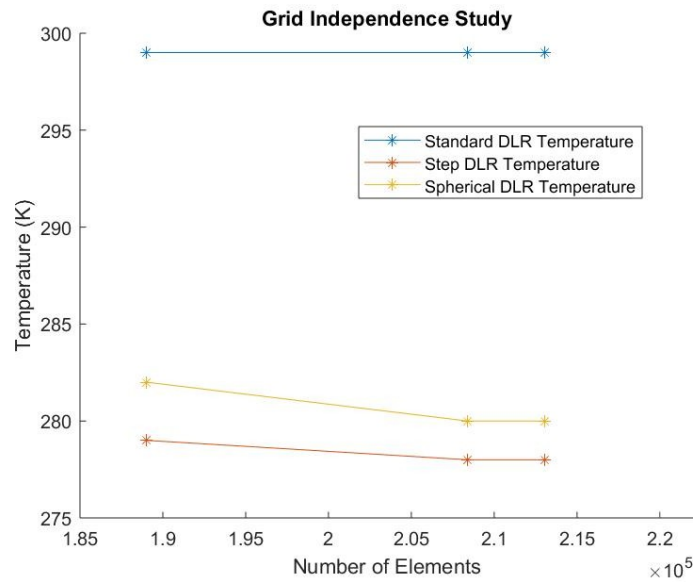


Figure 6: Grid independence study

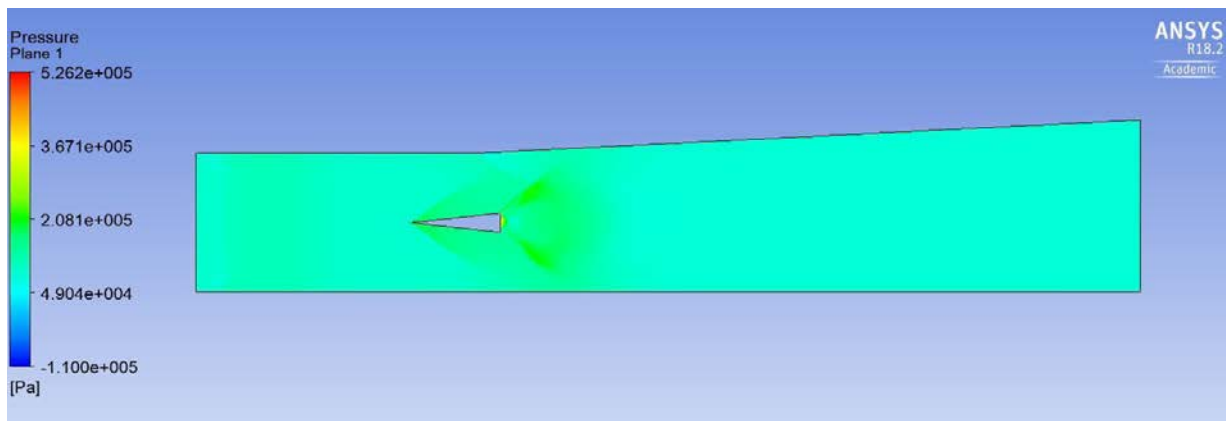
2. Results and Discussion

2.1 Results

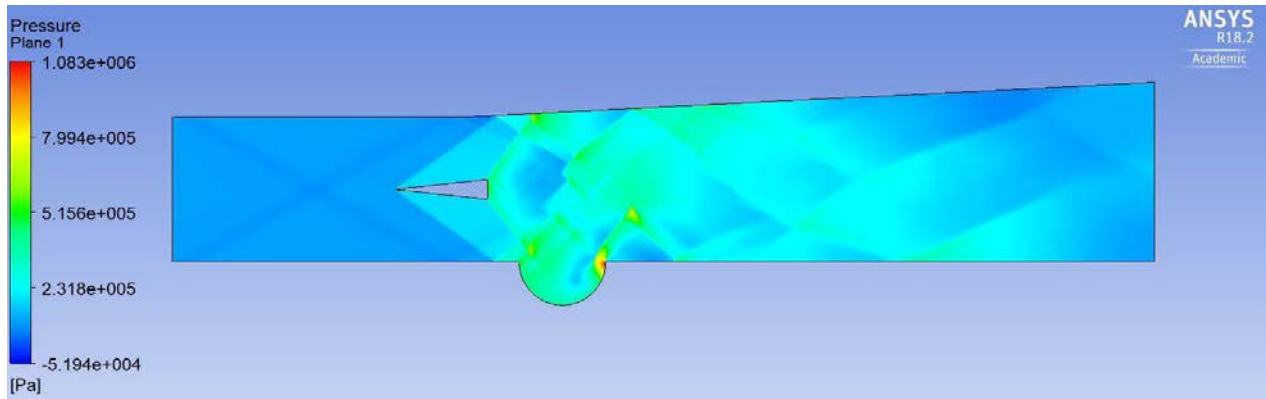
As discussed in the first part of the project, the critical parameters which give a clear picture of the flow are pressure, density, velocity and temperature. The observation made from the first part of the project is, the oblique shock waves are generated from the leading edge of the fuel struts at the walls of the combustion chamber and they were experiencing multiple reflections. By these reflections, the shockwaves form a multiple numbers of shockwave trains at the end of the strut. These trains are helpful for efficient of mixing of fuel and air.

From the first part of the project, it was clear that by using cavity-based combustion chambers there was an increase in residence time and mixing capability of the combustion process. Among the three models, step cavity design generated a good number of shock waves which results in getting good mixing rate.

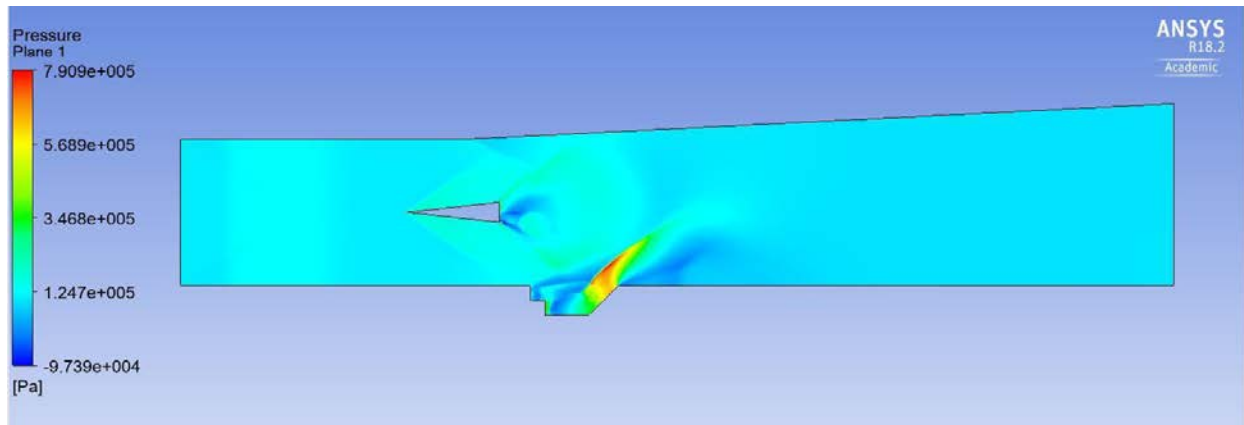
For the present project, the mesh was refined with a good number of node points than the previous mesh to get more accurate solution. Now the results are going to compare with the previous results. The below figures are the contours of pressure, temperature, density and velocity.



a)

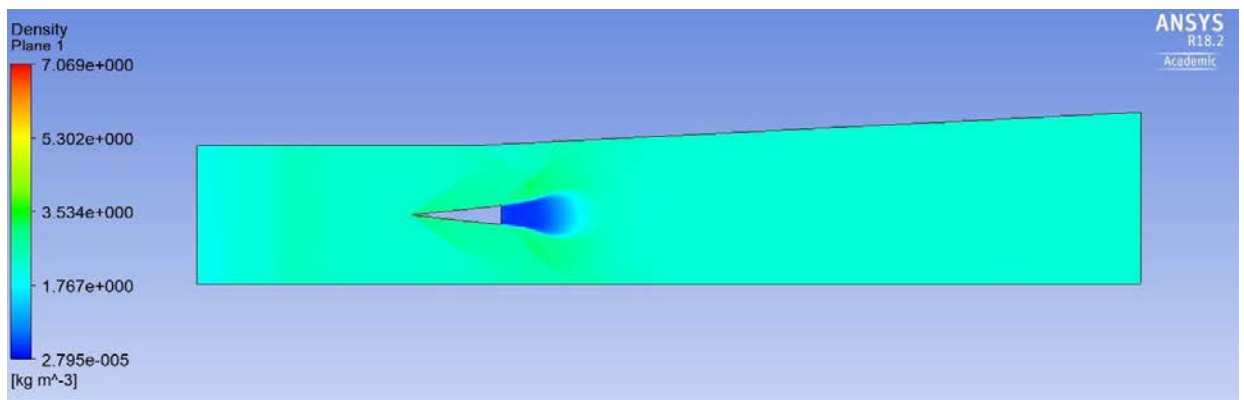


b)

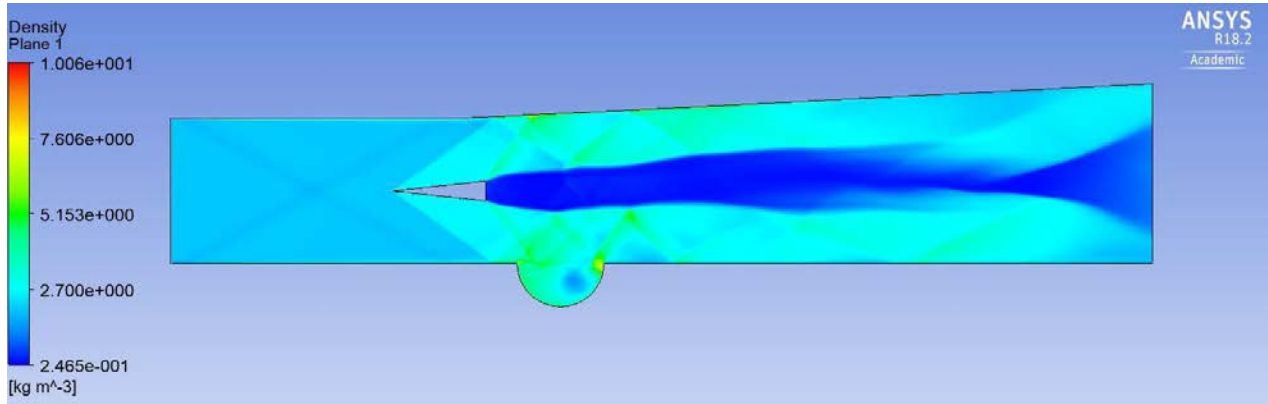


c)

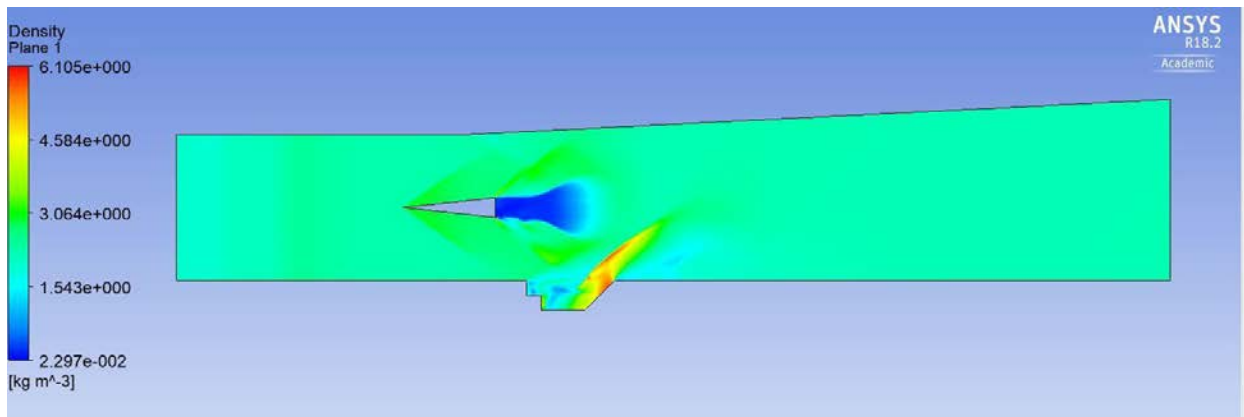
Figure 7: Pressure Contours of a) Standard DLR scramjet, b) Spherical cavity and c) Step cavity



a)

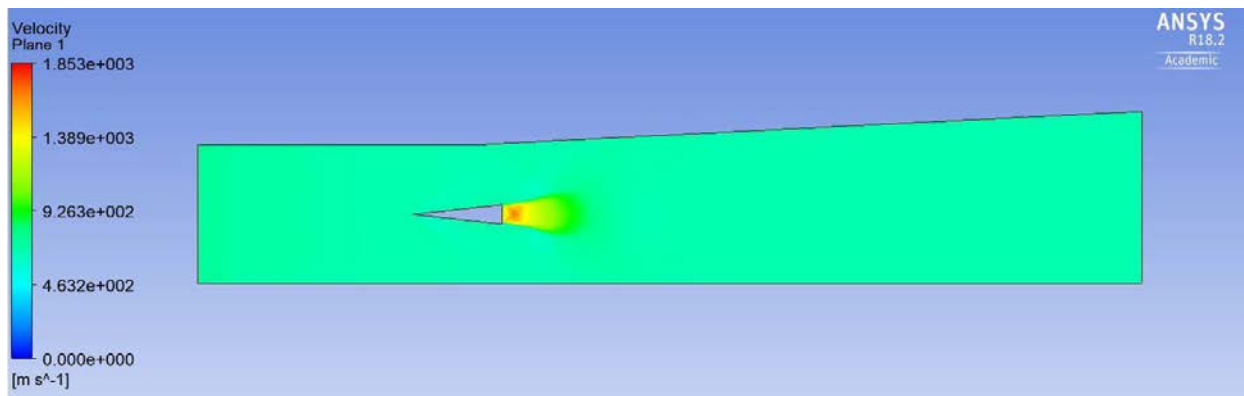


b)

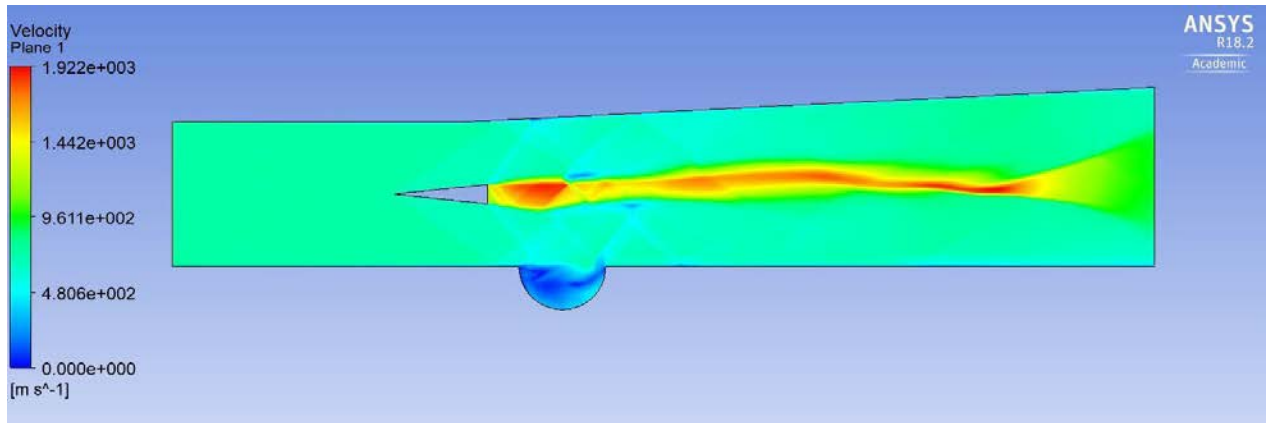


c)

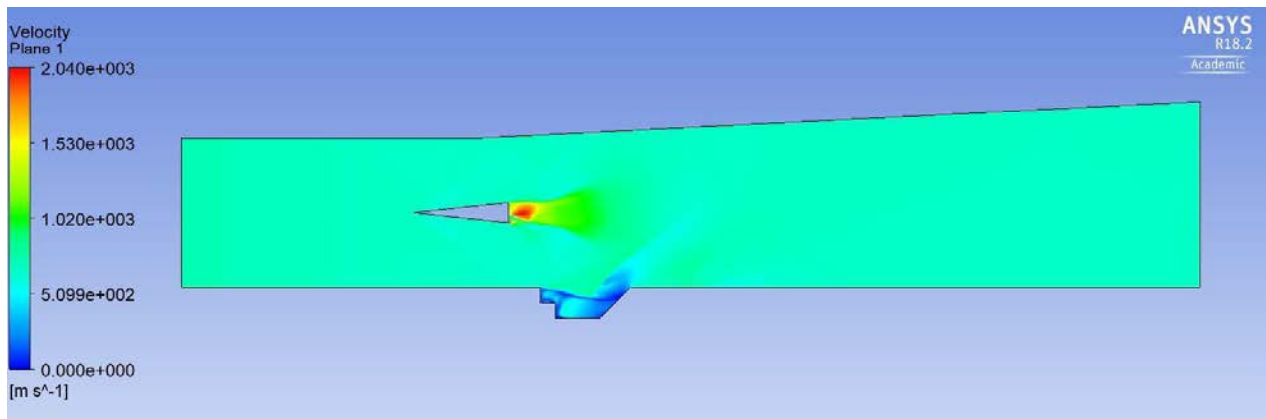
Figure 8: Density Contours of a) Standard DLR scramjet, b) Spherical cavity and c) Step cavity



a)

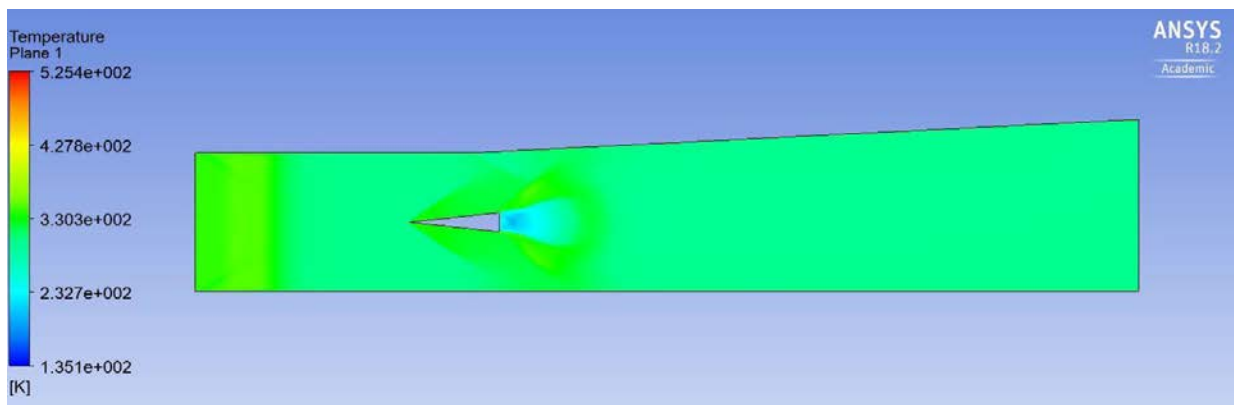


b)

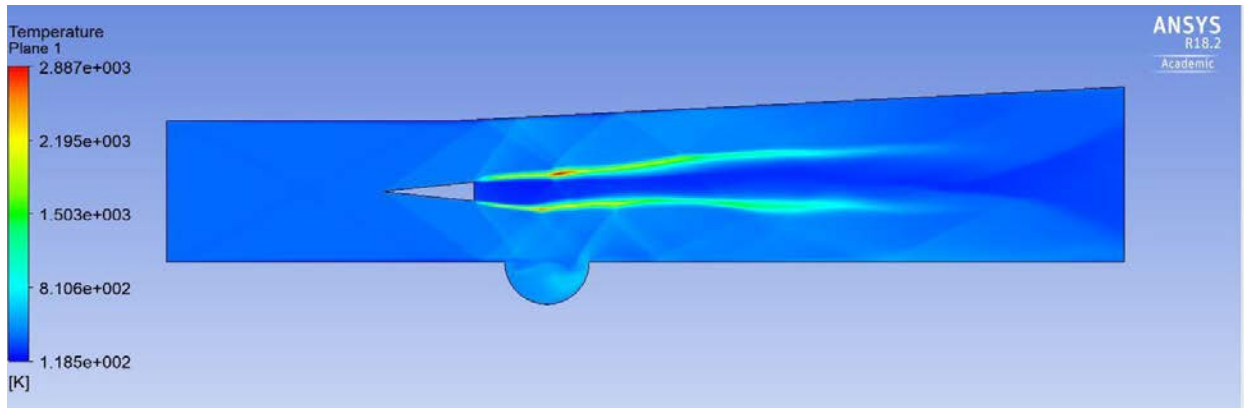


c)

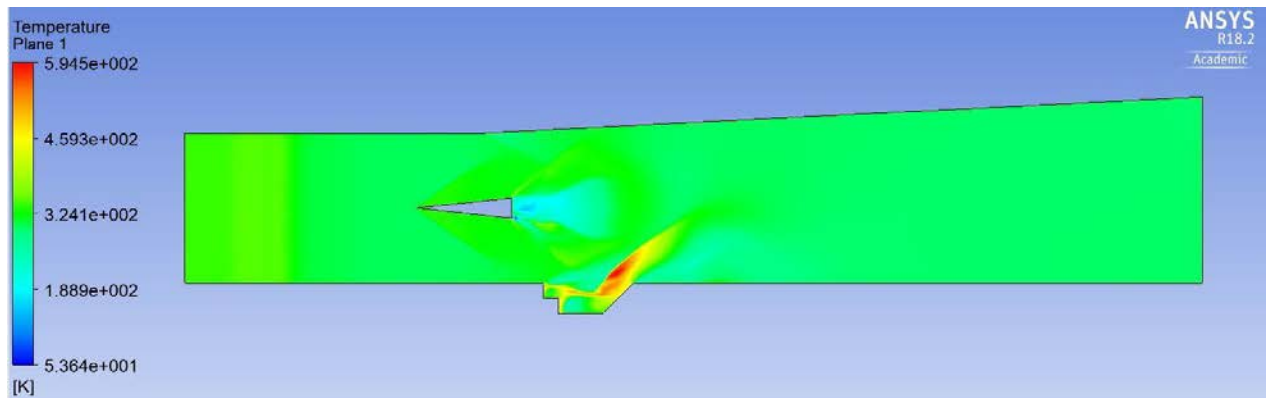
Figure 9: Velocity Contours of a) Standard DLR scramjet, b) Spherical cavity and c) Step cavity



a)



b)



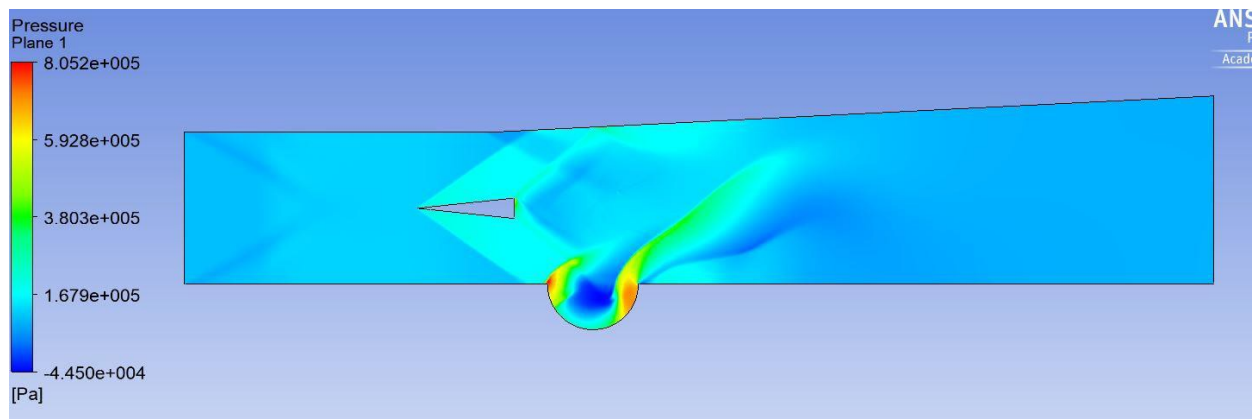
c)

Figure 10: Temperature Contours of a) Standard DLR scramjet, b) Spherical cavity and c) Step cavity

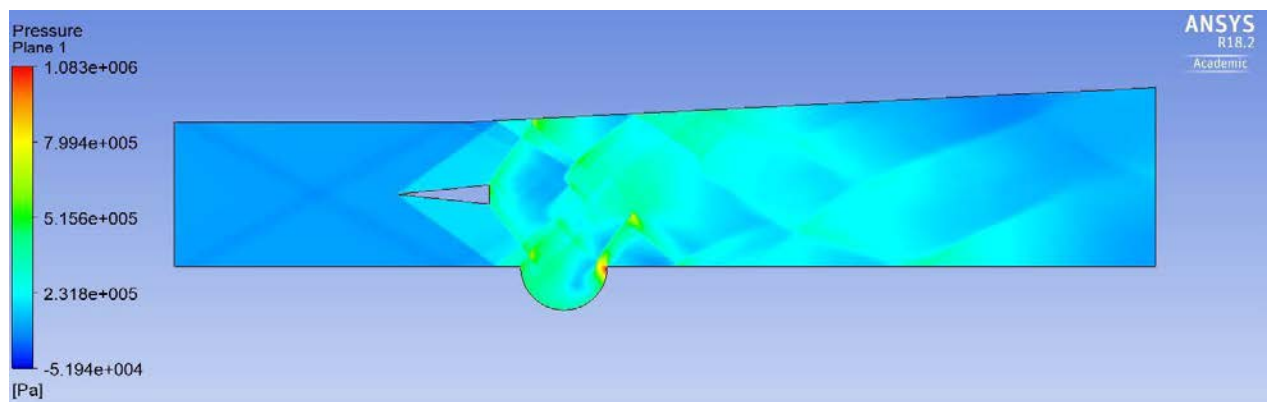
By observing Figure 7, oblique shock waves are generated from the leading edge and form a shockwave train. From above figure, the step and spherical cavity-based model combustion chambers have more recirculation zones and shock waves. These results in increasing the residence time of air in the combustion chamber which is a major parameter in mixing efficiency. From Figure 8, Behind the fuel strut, there is a huge wake zone for the DLR scramjet and very less wake zone for the cavity-based scramjets is observed.

2.2 Comparison of Results

As per theory, the accuracy of the result depends on the refinement of the mesh. In this section, the effect of mesh refinement is going to be explained by taking the spherical cavity model as a reference. The minimum size of the mesh taken in the first part of the project is 0.3mm and for the second part of the project is 0.05 mm. By changing the minimum face size, the number of mesh elements gone up to 210000 which is four times higher than the previous mesh elements. The below figures show the effect of mesh refinement clearly.



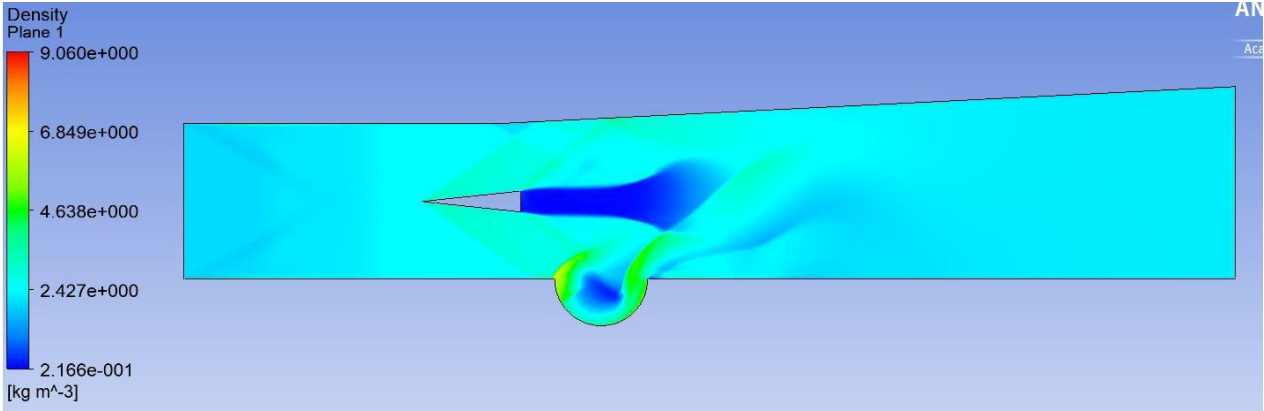
a)



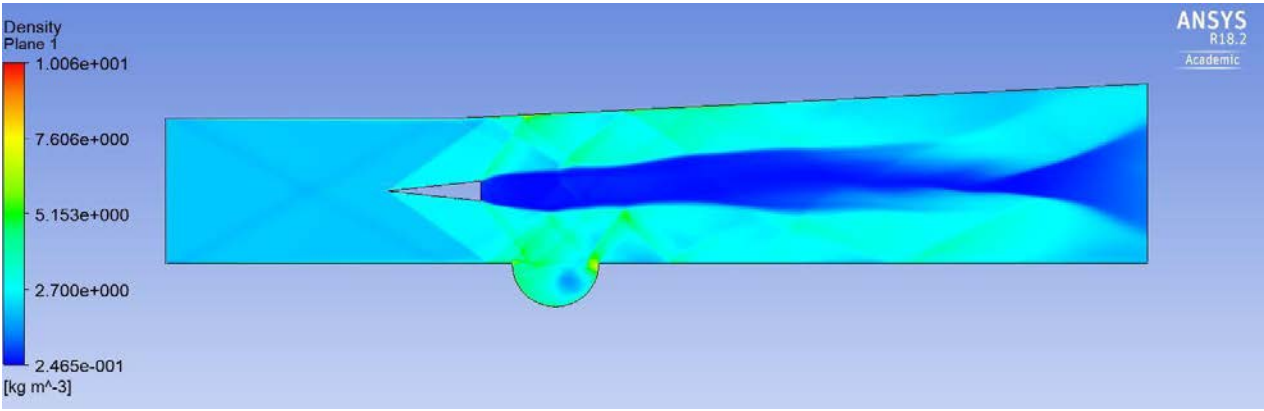
b)

Figure 11: Pressure contours of spherical cavity Scramjet Combustion chamber with a) Regular Mesh and b) Refined mesh

From Figure 11, by simulating with refined mesh the visibility of the shock waves and shock wave train formation is high. The multiple reflections of shock waves can be observed clearly. The legend (scale limits) clearly shows the pressure values. The values of pressure are refined with the new mesh. Therefore, the result was accurate with the new mesh.



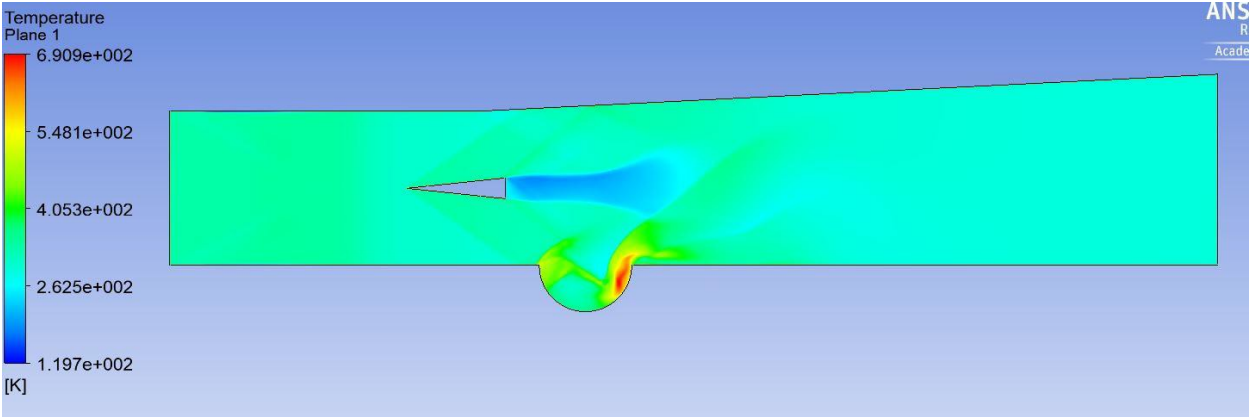
a)



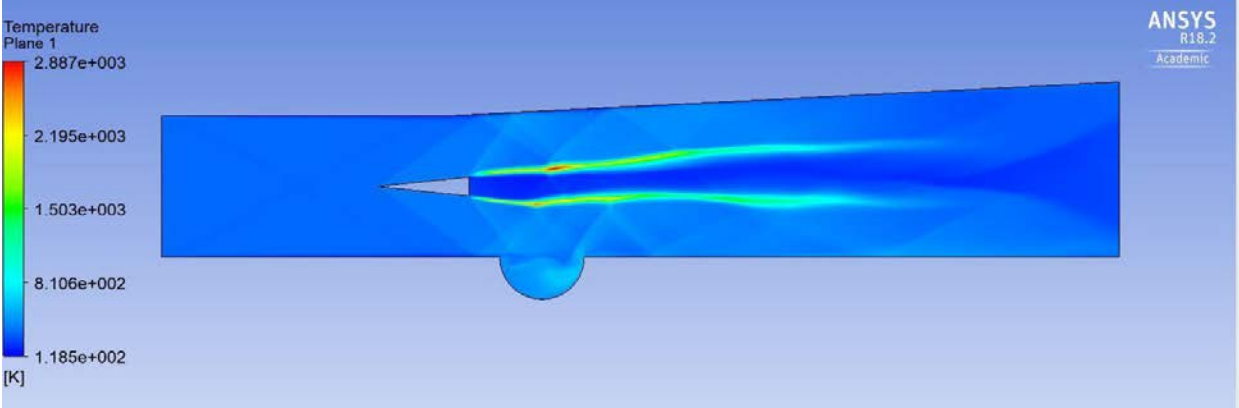
b)

Figure 12: Density contours of spherical cavity Scramjet Combustion chamber with a) Regular Mesh and b) Refined mesh

From the Figure 12, it is clear that there is a huge wake zone behind the fuel strut mechanism. In the regular mesh model, the mixing was observed at around 160mm but in case of refined mesh slight mixing was observed at around 300mm.

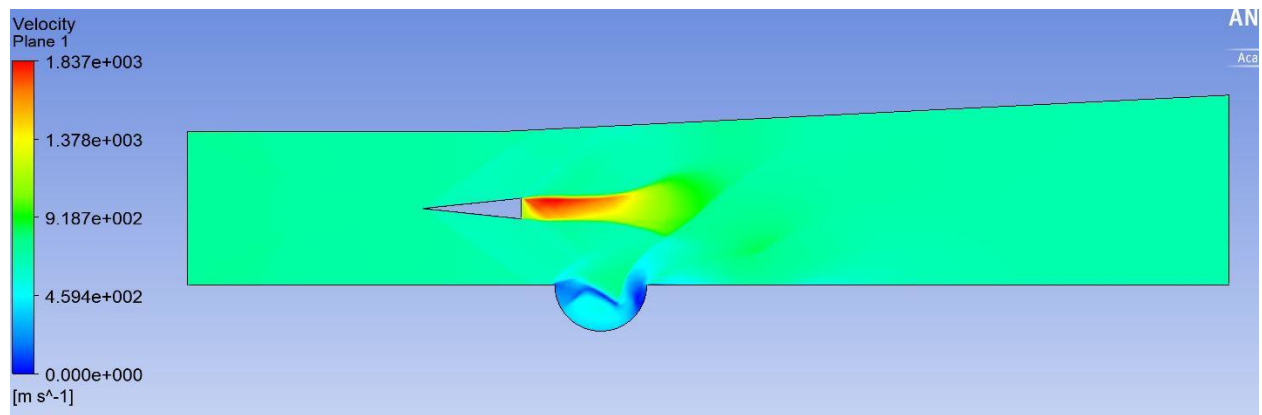


a)

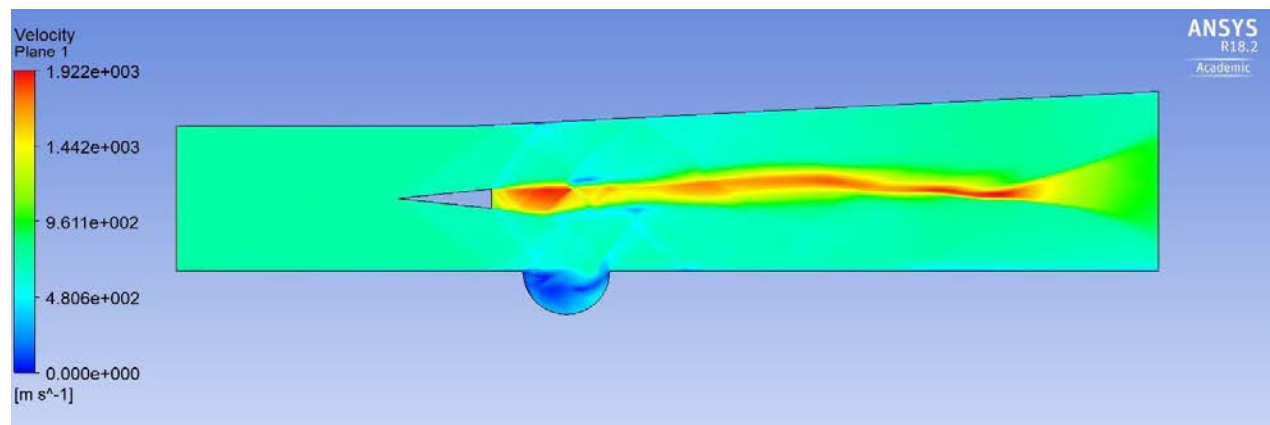


b)

Figure 13: Temperature contours of spherical cavity Scramjet Combustion chamber with a) Regular Mesh and b) Refined mesh



a)

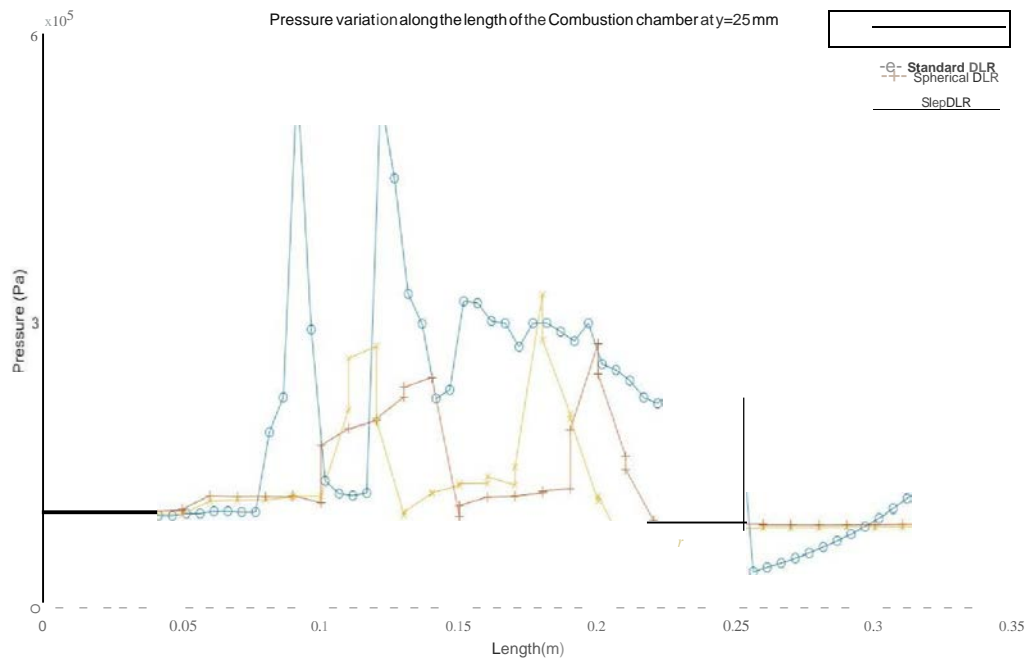
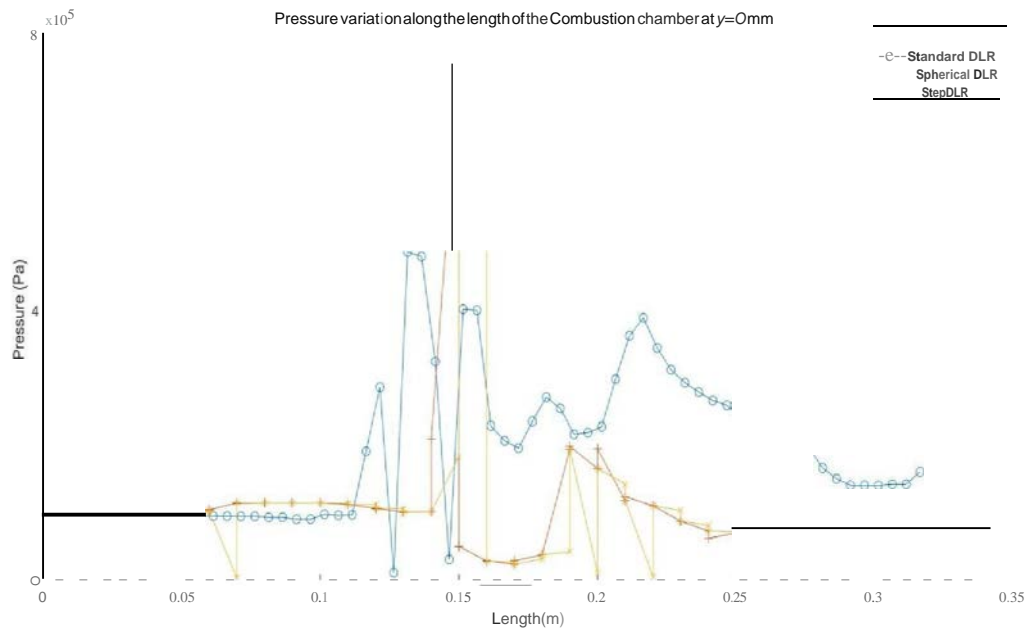


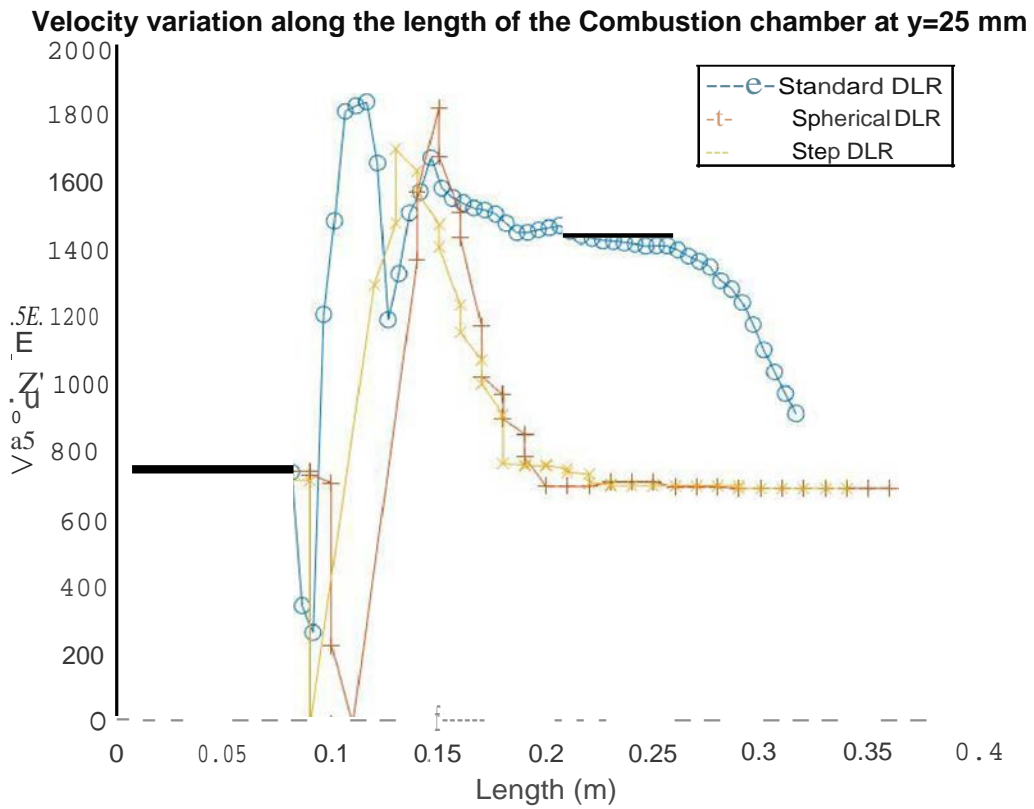
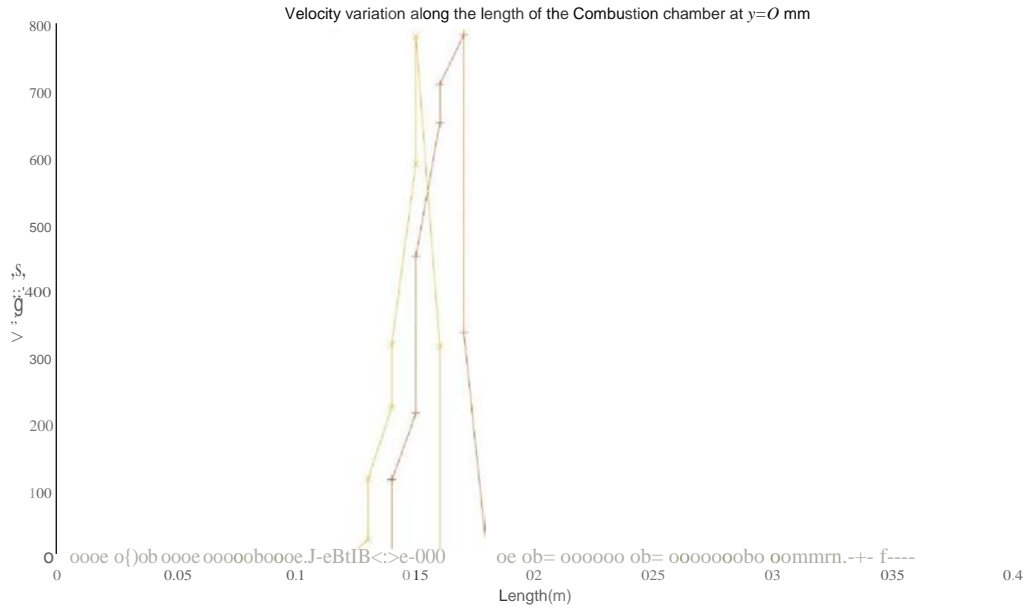
b)

Figure 14: Velocity contours of spherical cavity Scramjet Combustion chamber with a) Regular Mesh and b) Refined mesh

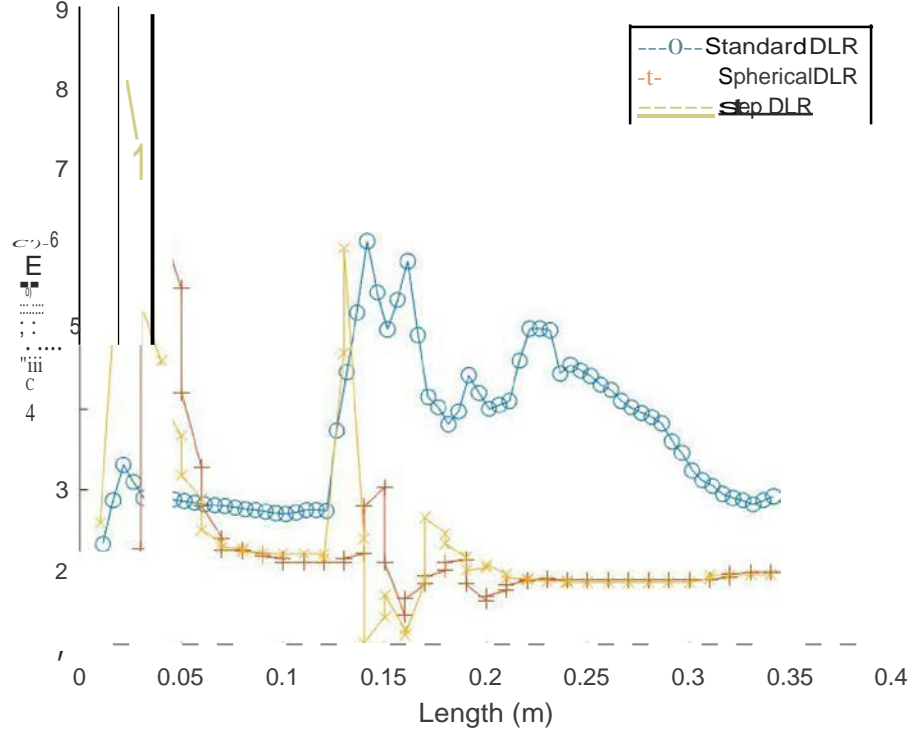
From Figure 14, accuracy of the temperature profile is more in the refined mesh model than the regular mesh model. By observing figure, the velocity behind the fuel strut is very high up to 160mm in the regular mesh model but in case of refined mesh, it is high up to 300mm. This shows the use of refined meshing analysis.

Along with the contours; pressure, temperature, density and velocity profiles along the length of the combustion chamber and a cross stream of the combustion chamber are also going to be compared with regular mesh profiles.

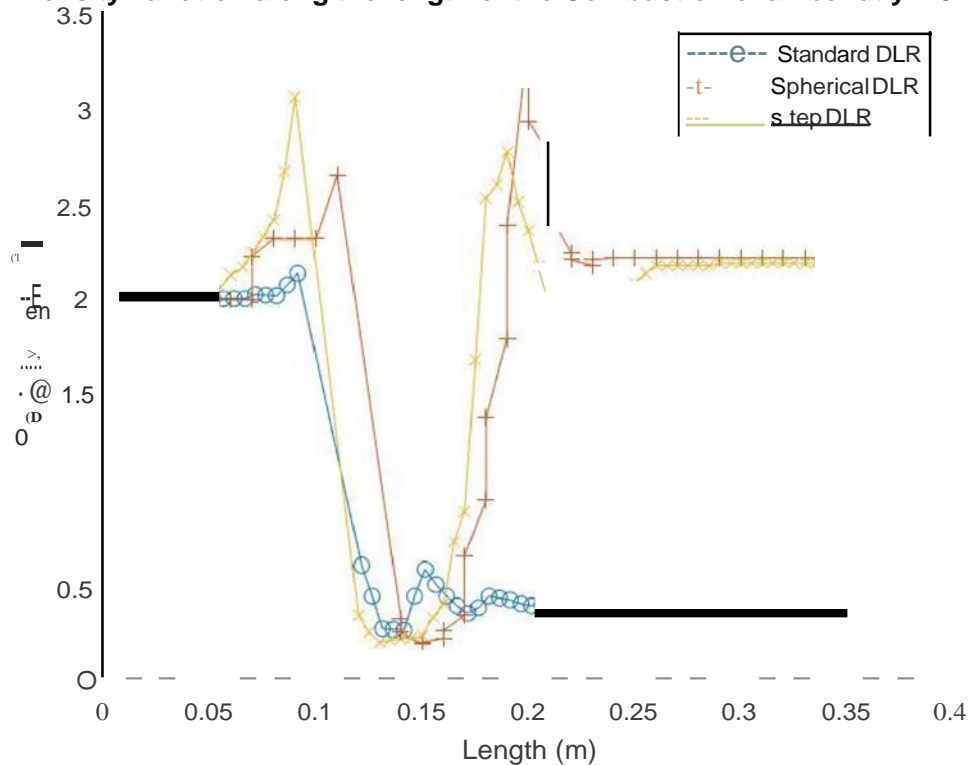




Density variation along the length of the Combustion chamber at y=0 mm



Density variation along the length of the Combustion chamber at y=25 mm



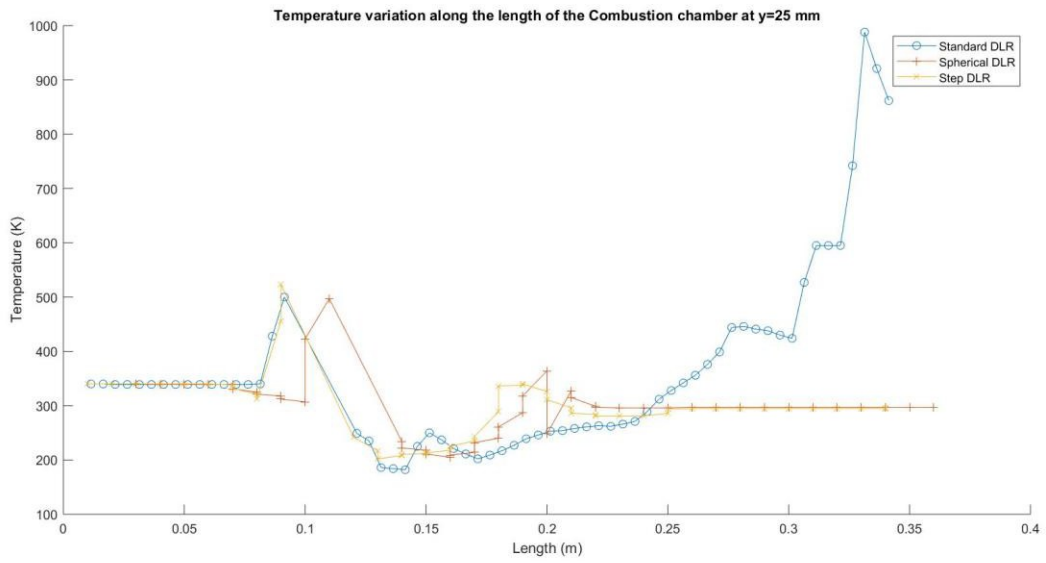
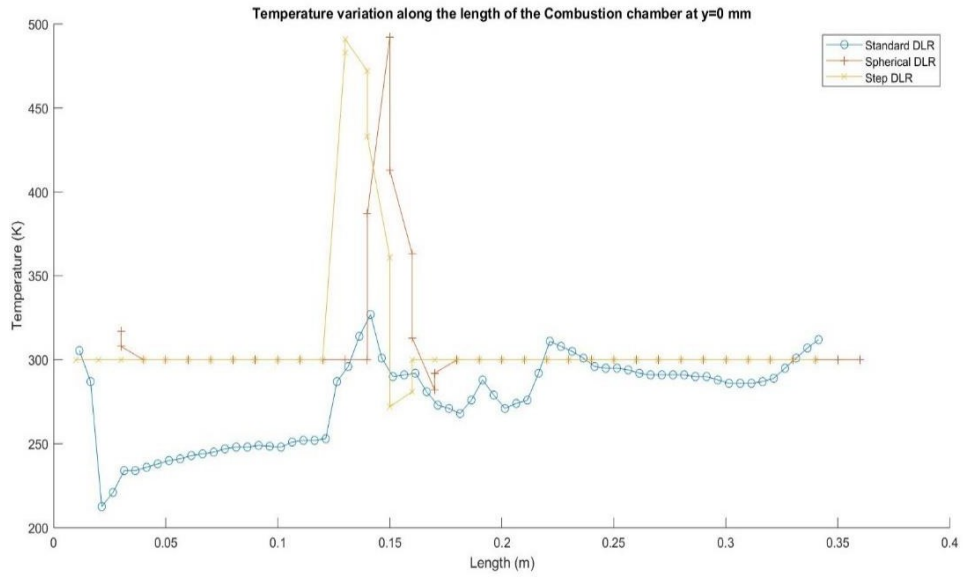
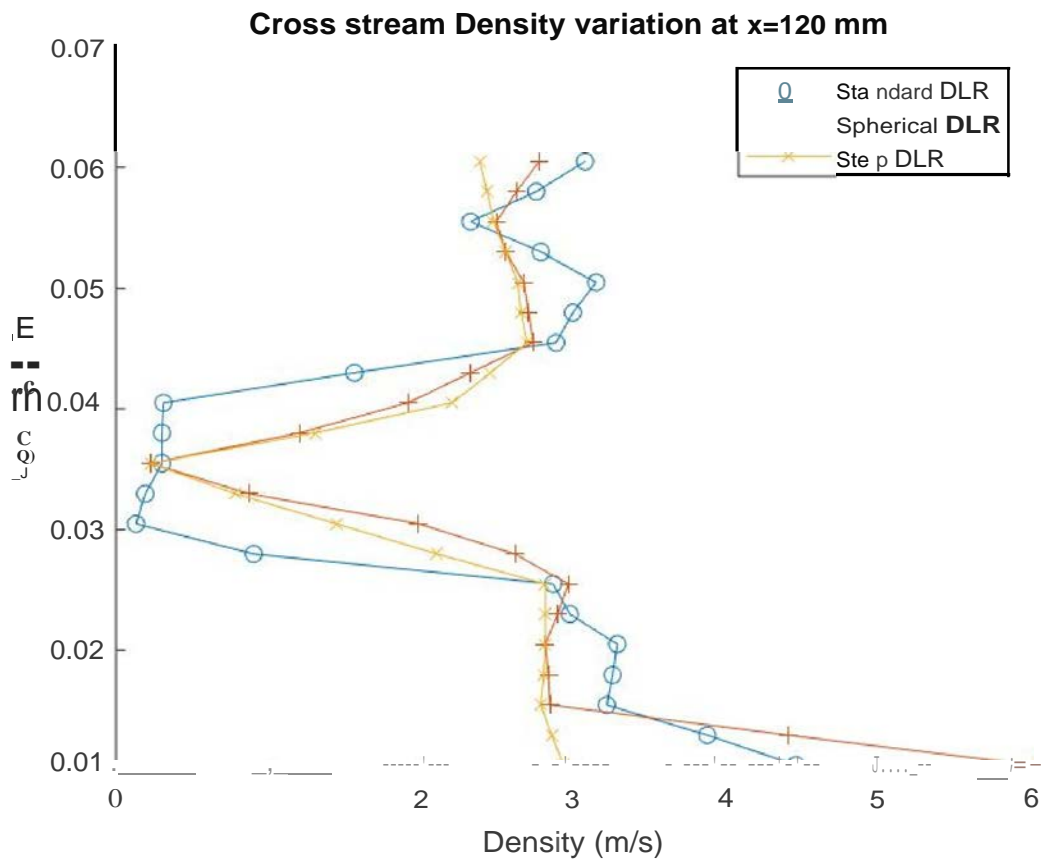
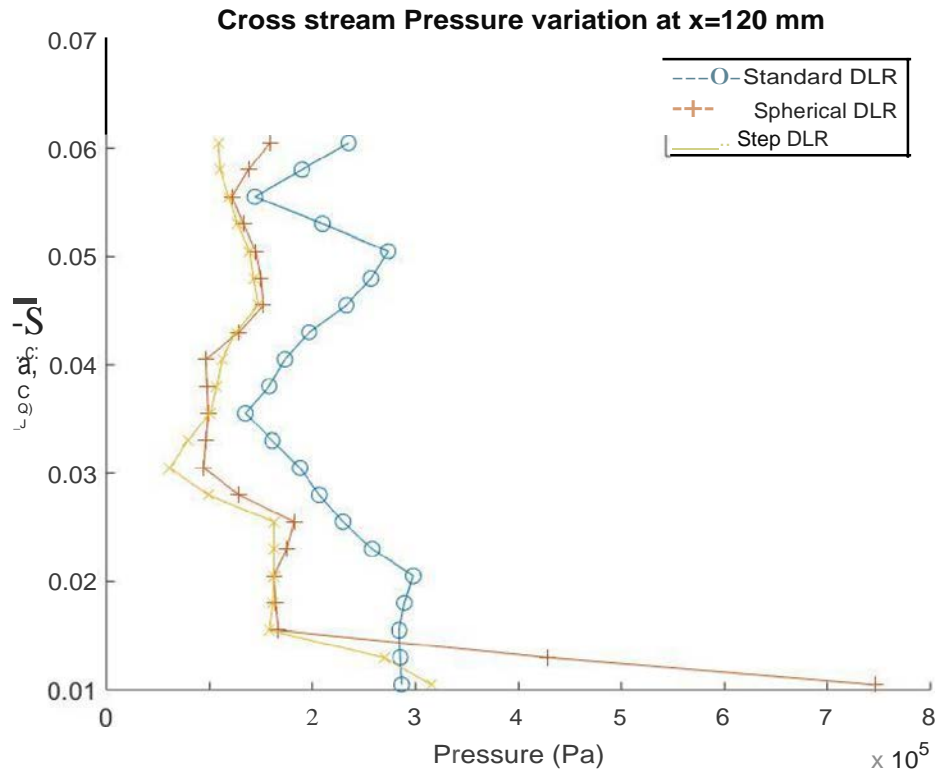
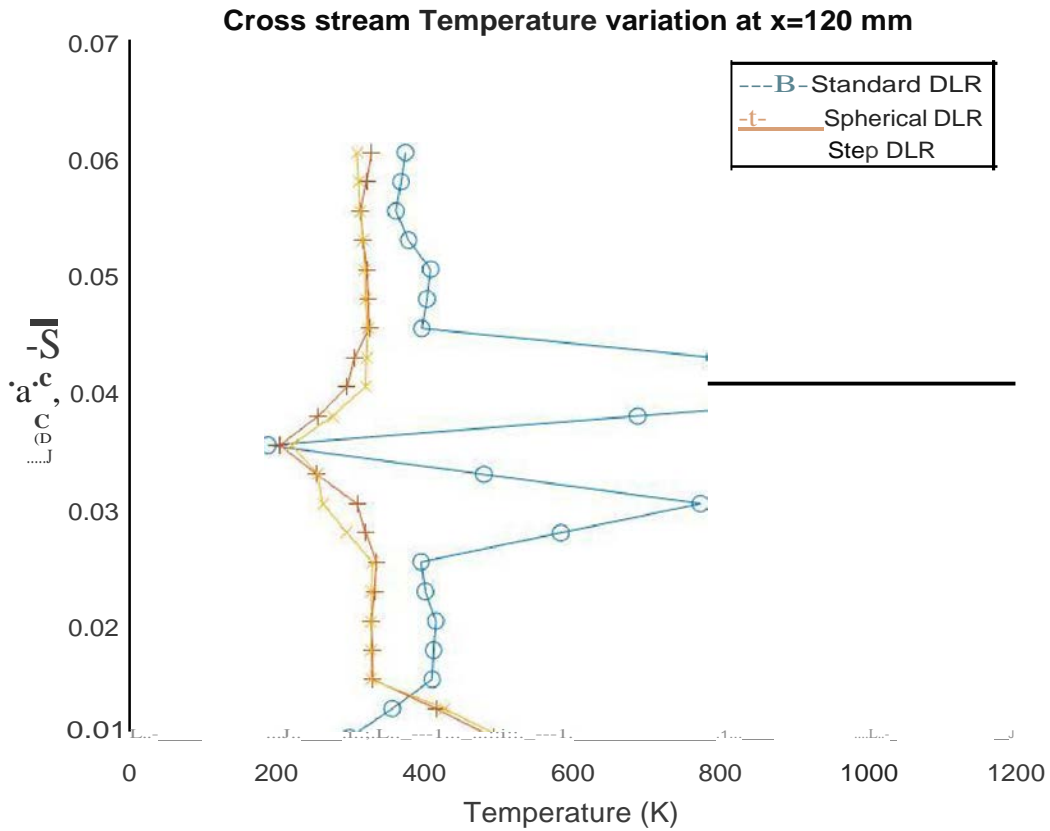
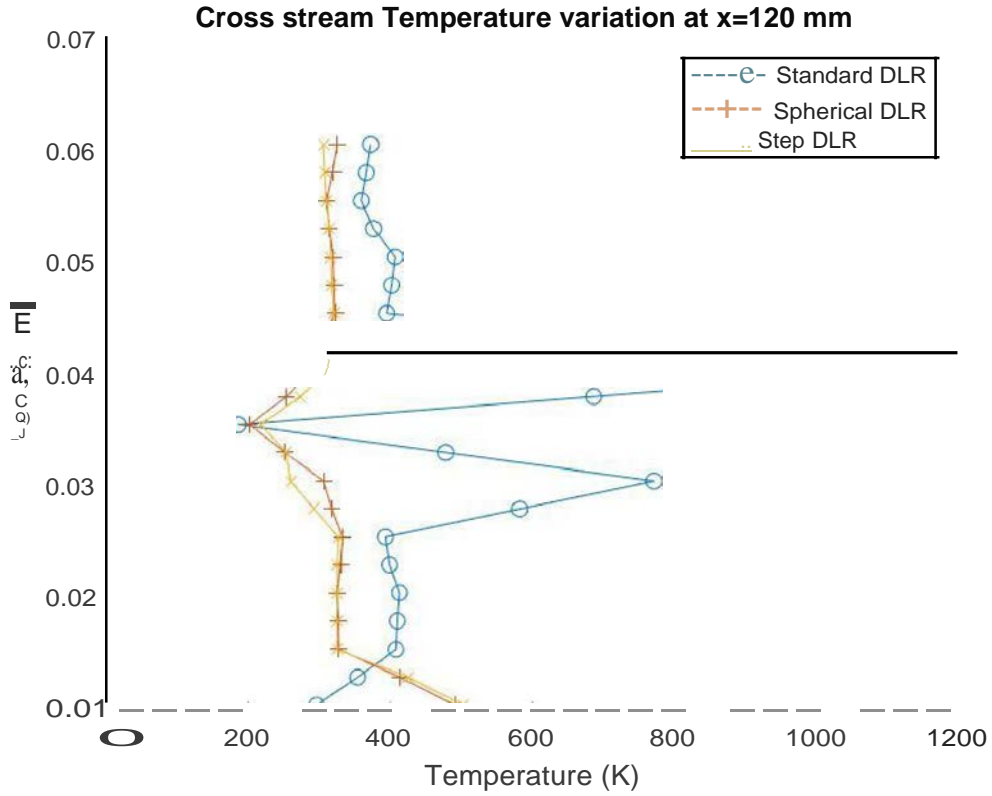
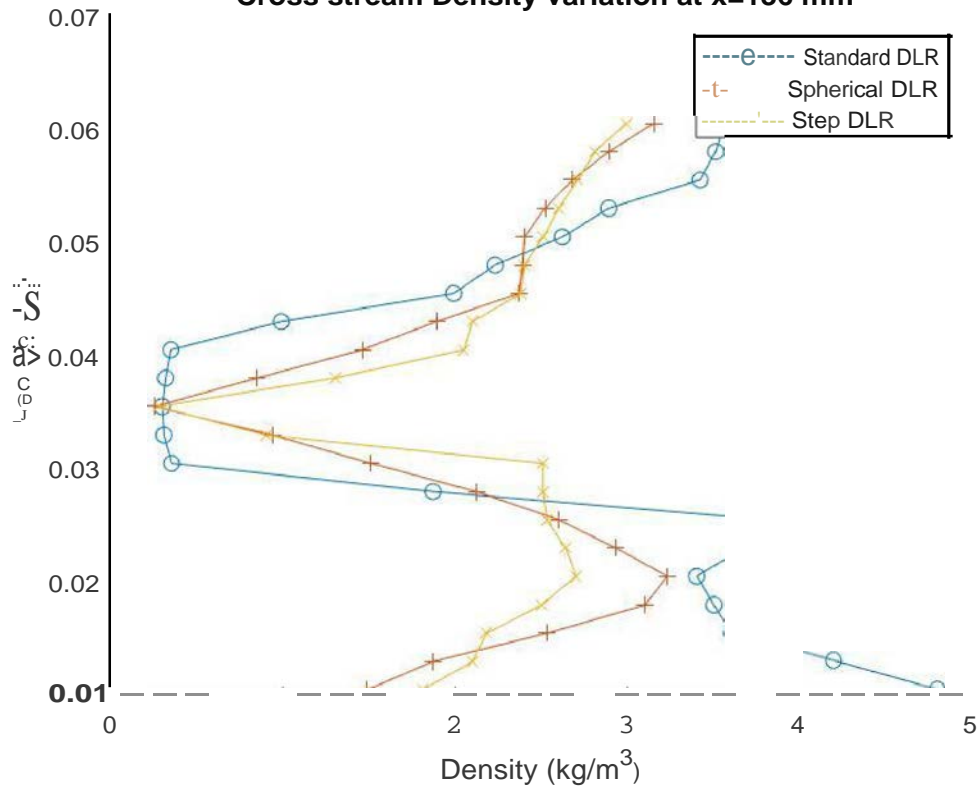


Figure 15: Pressure, Velocity, density and Temperature profiles along the length of the combustion chamber

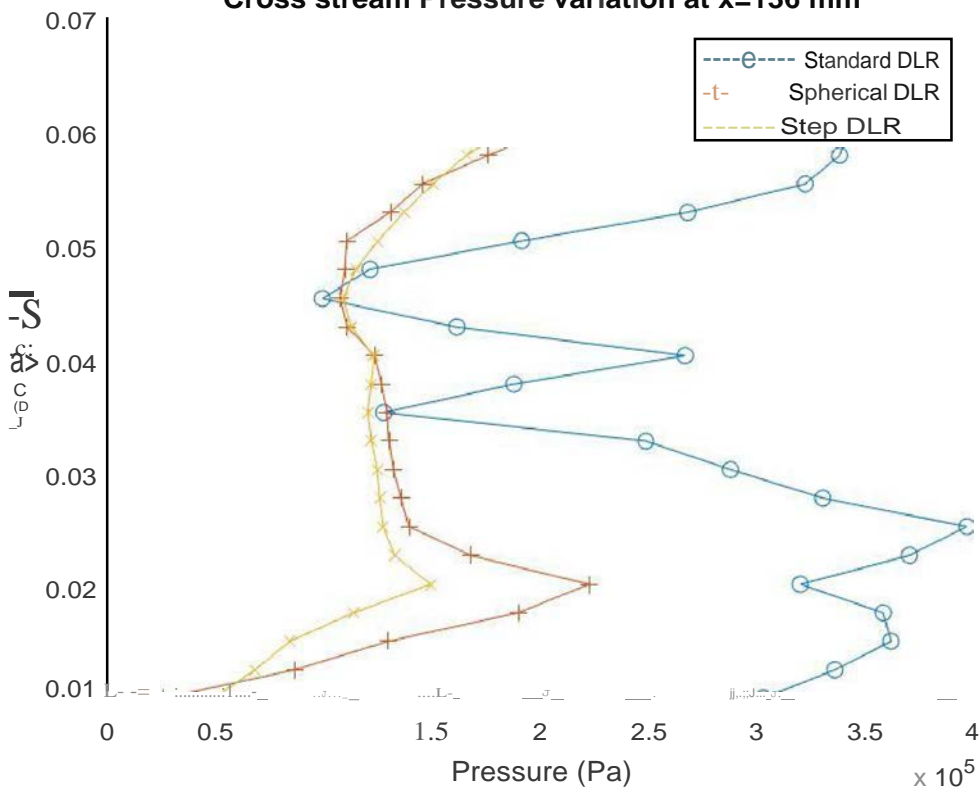


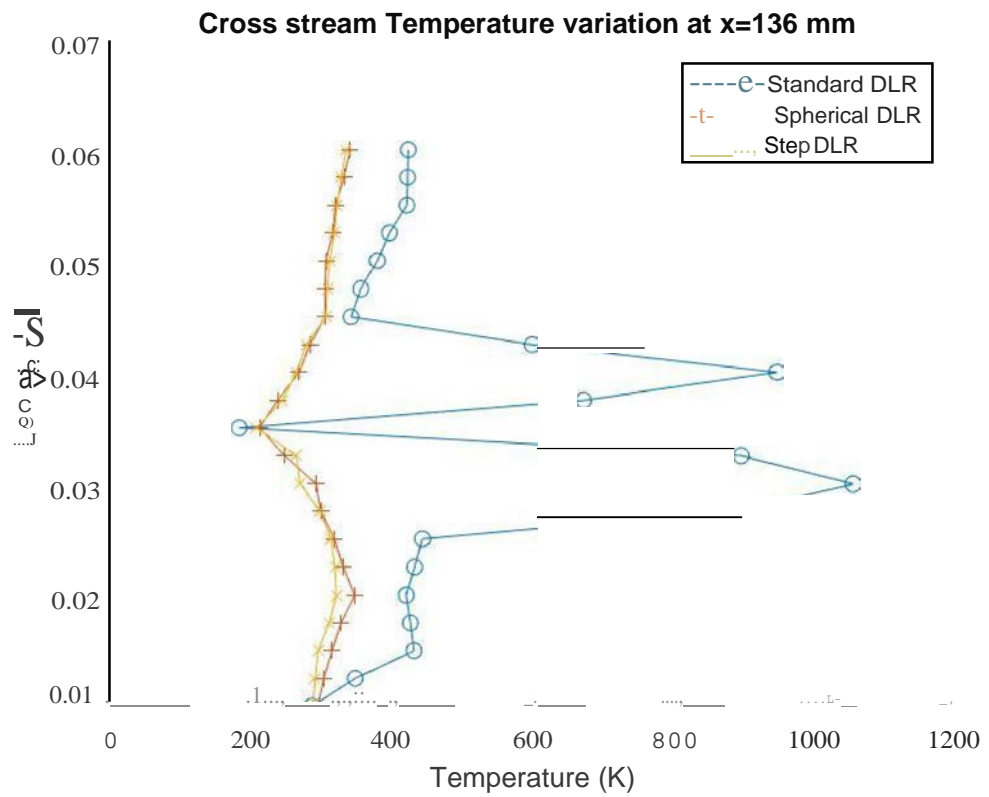
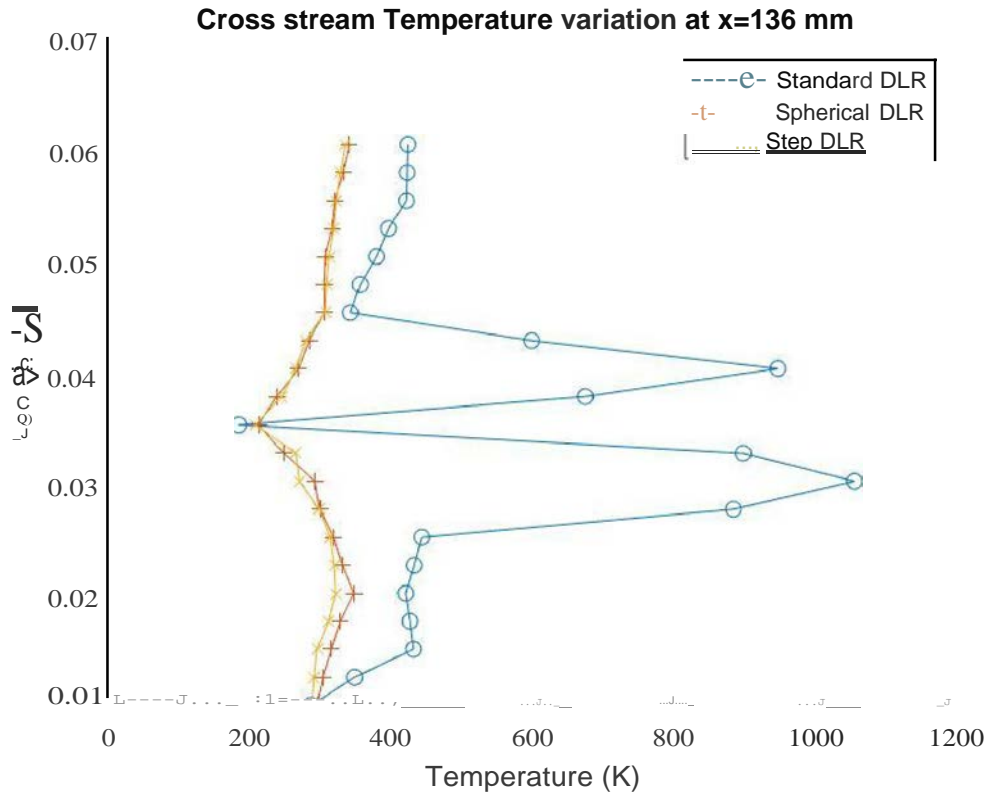


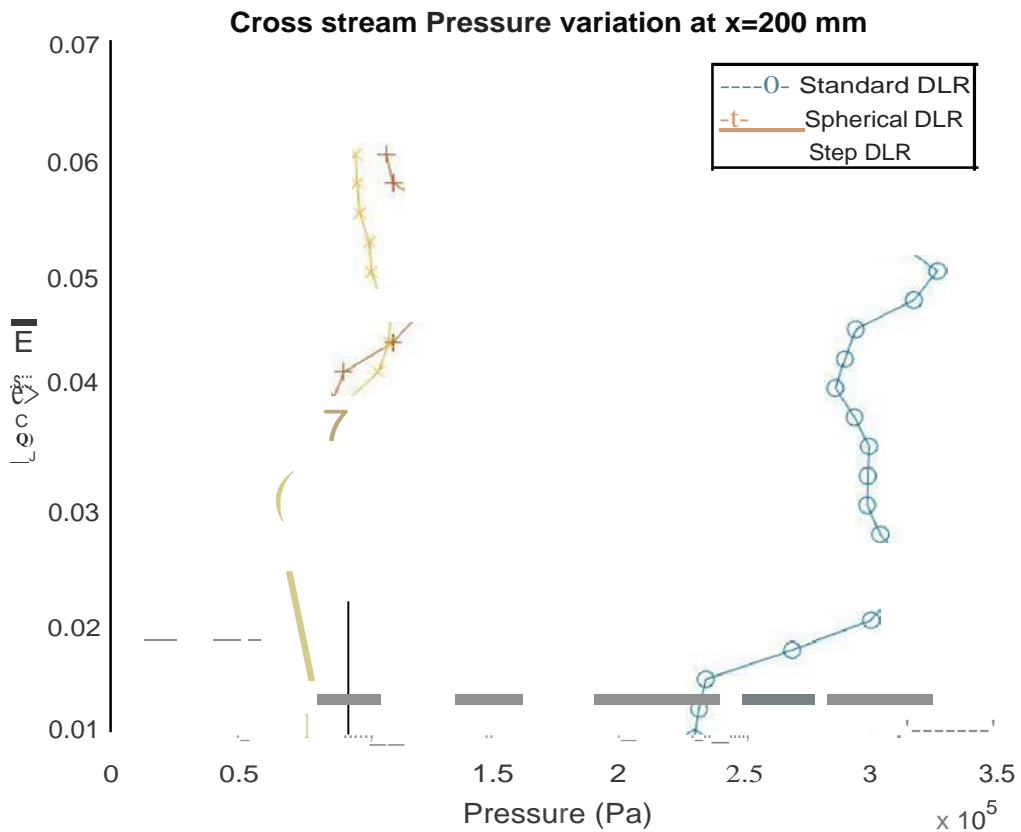
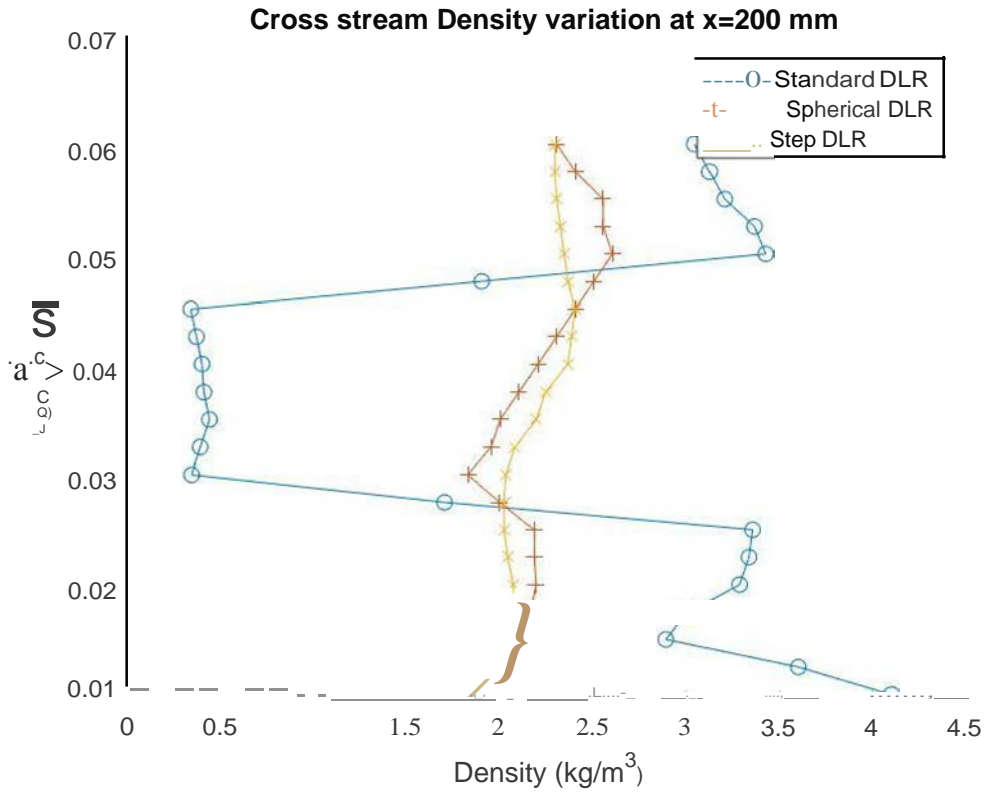
Cross stream Density variation at x=136 mm



Cross stream Pressure variation at x=136 mm







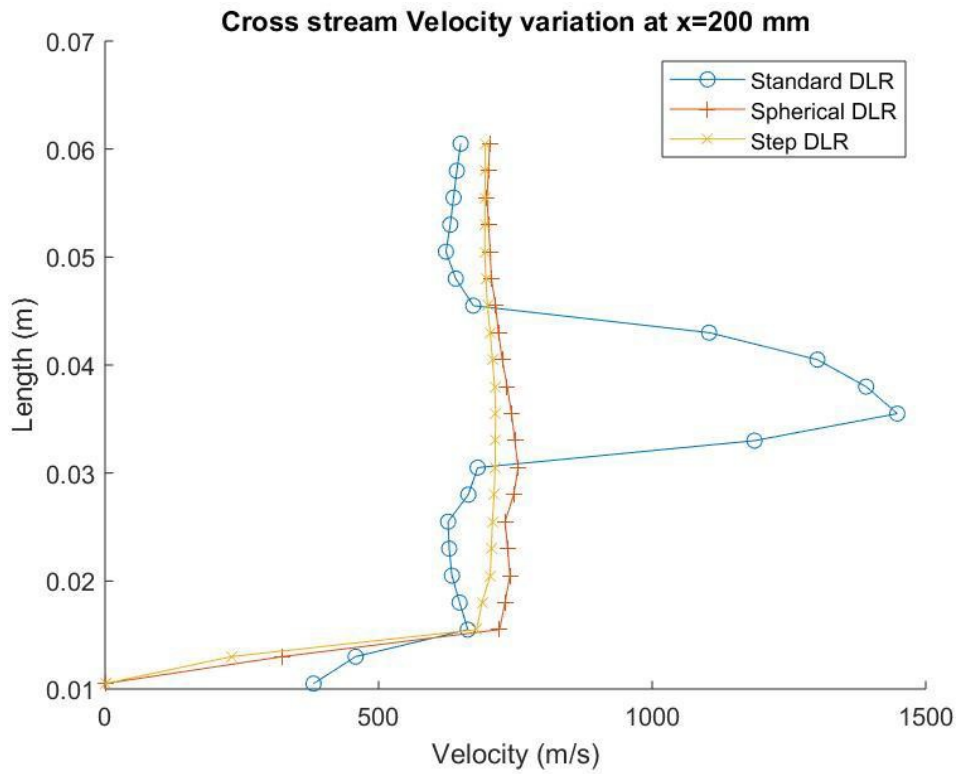
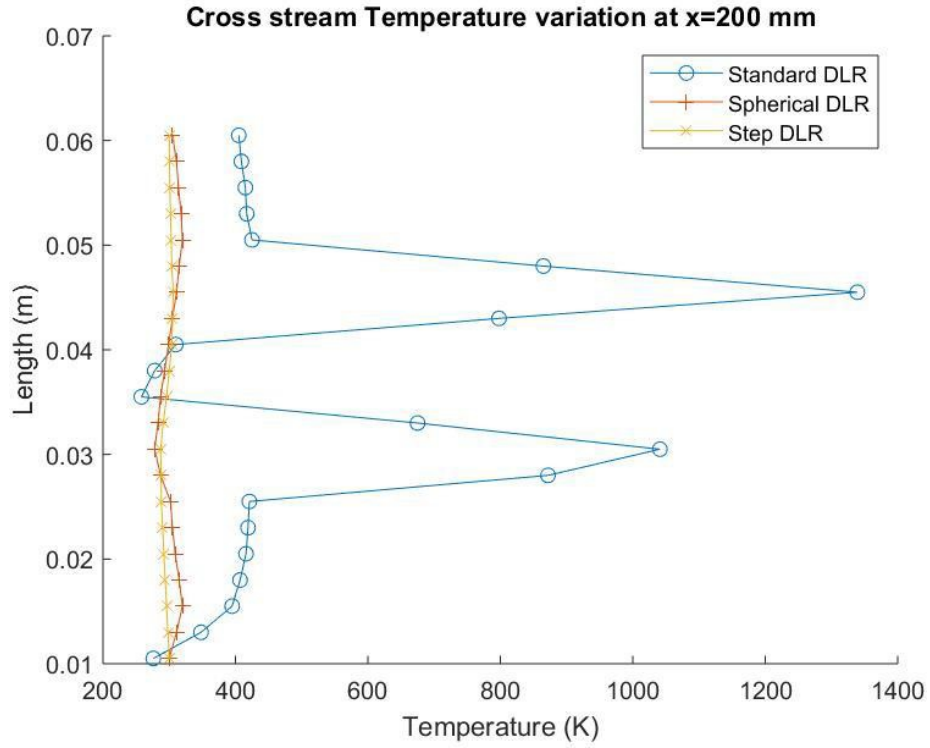
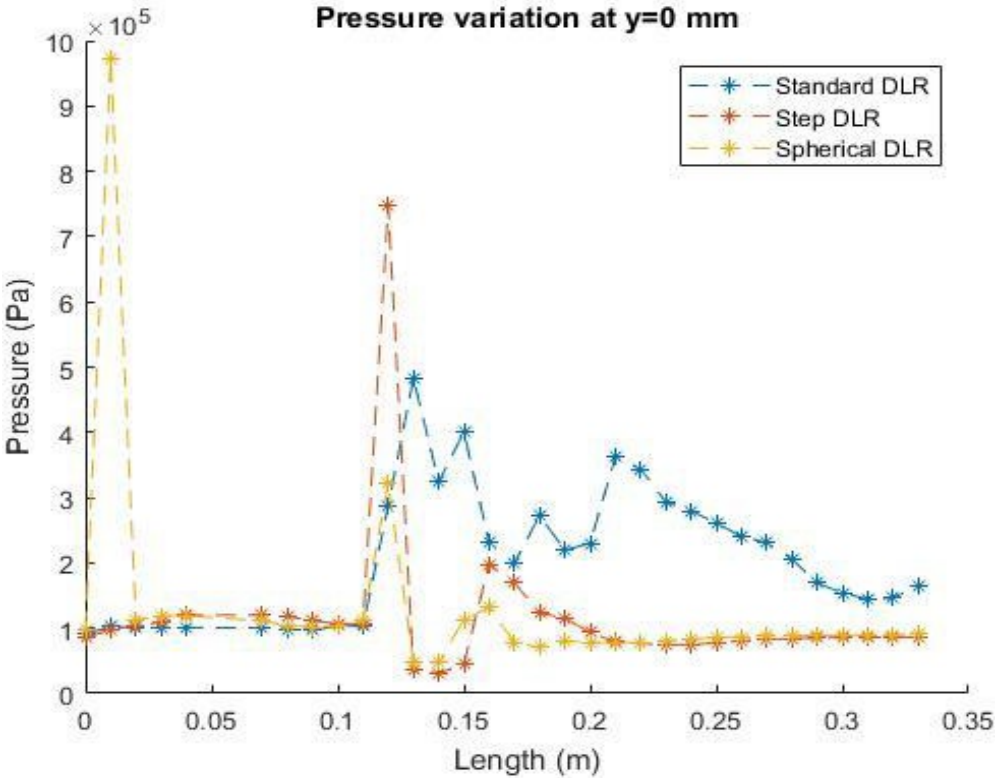
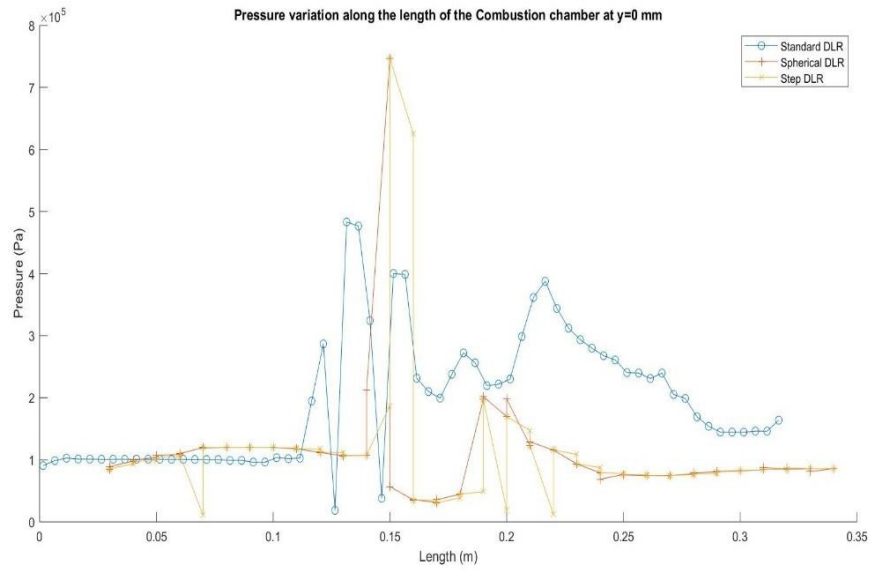


Figure 16: Pressure, Density, Velocity and Temperature profiles cross stream of the combustion chamber

The above are the pressure, temperature, velocity and density profiles along the length of the combustion chamber at $y=0\text{mm}$ and $y=25\text{mm}$. Now the plots are going to be compared with the regular mesh plots. For simplicity, pressure plots are only going to be compared.

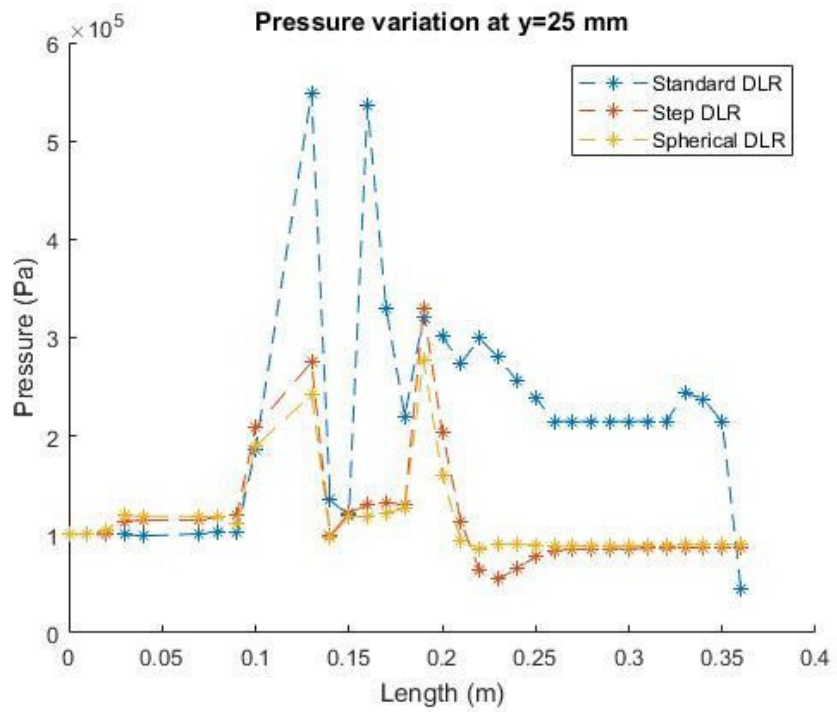


a)

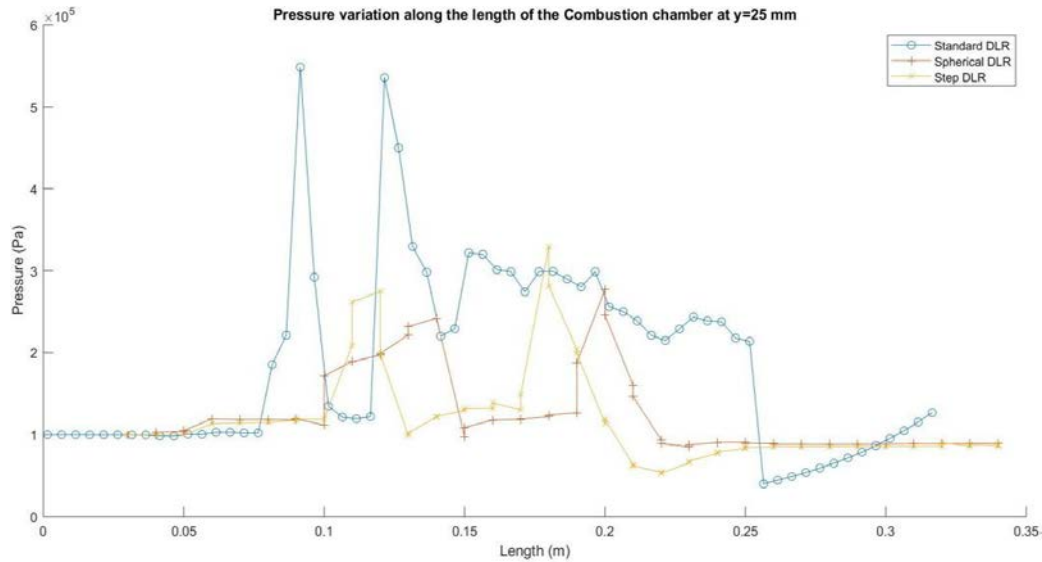


b)

Figure 17: Pressure variation along the length of the combustion chamber at y=0mm with a) Regular mesh and b) Refined mesh



a)



b)

Figure 18: Pressure variation along the length of the combustion chamber at $y=25\text{mm}$ with a) Regular mesh and b) Refined mesh

From the above plots, the refined mesh solution is a bit accurate than the previous solution. But, in the case of cavity-based combustion chambers, the pressure profile is a bit different than the previous solution. In the regular mesh solution, the step and spherical cavity have a similar profile but in case of refined mesh solution, there is a small difference.

2.3 Conclusion

The modelling and simulation of scramjet combustion chambers with cavity-based (step and spherical) fuel strut mechanism with refined mesh have been done in ANSYS Fluent software using SST k-omega model, RANS equations and finite rate eddy dissipation model. The main purpose of the project is to introduce a new design for the combustion chamber to increase the efficiency of mixing and most effective use of fuel. To achieve that spherical and step cavity flame holding mechanisms were introduced in the

combustion chamber. These models were tested in ANSYS Fluent software. In the first part of the project, these cavity-based models tested with the minimum size of the mesh 0.3mm. Through that, it was found that the step cavity gives better result compared to the other two models. In this project, the same models and same boundary conditions were used for simulation. But, the only difference between the first part and second part is meshing size. As per the theory, refined mesh will give the accurate result. That means the accuracy of the result depends on the meshing elements. In the present part of the project, models were tested with a minimum size of 0.05mm wherein the first part the models were tested with 0.3mm mesh. Therefore, the number of elements presented in the second part of the project is around 210000 wherein the first part it was around 50000 only. By simulating with a greater number of elements, the visibility of shock waves, shock wave train formation, wake zones were increased. By comparing the results of first part and second part of the project it was found that the solutions were almost same. But, accuracy of the result obtained in the second part of the project is more.

Modelling and Simulation of Scramjet Engine with different Inlets

1. INTRODUCTION

1.1 Theory

The main purpose of the diffuser/inlet is to compress air. For regular jet engines, the inlet works along with the mechanical compressor. But, in scramjet engines inlet alone itself works as an inlet and compressor. Since the air is in high speed, there is no need to use an additional compressor for scramjet engines. To achieve good compression ratio, an efficient inlet design is required.

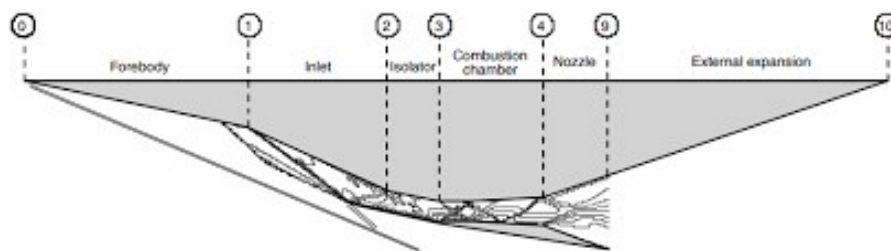
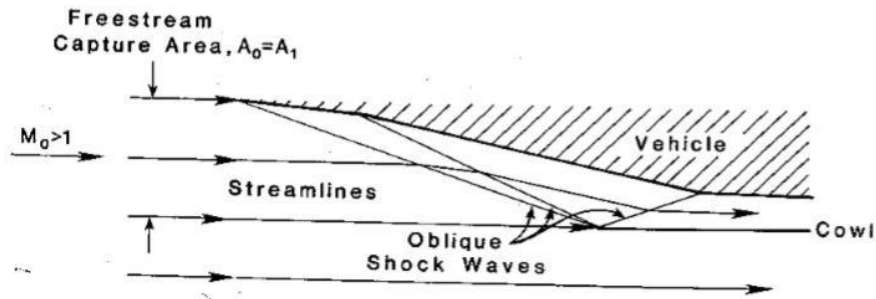


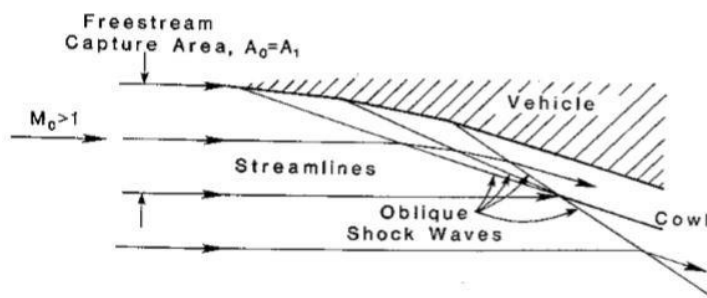
Figure 19: Flow stations in a Scramjet engine

There are three different types of inlets based on the compression process. Those are a) Internal compression, b) External compression and c) Internal and external compression. Figure 20 shows a rough sketch of these inlets. In external compression type inlets, the compression of the air takes place outside of the inlet due to the shock waves. The main disadvantage of the external compression inlet is it has more cowl drag compared to the other types. Figure 20b shows a rough sketch of internal and external compression inlet. In this type of inlet, the compression takes place outside as well as inside of the engine due to the shock waves. When it comes to the size, these types of engines are a bit longer

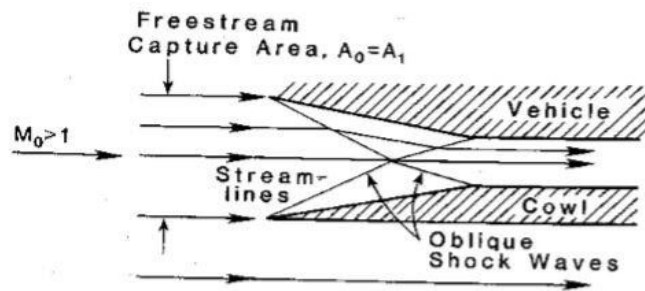
than the external compression engines. Figure 20c shows the internal compression type engine. In this type, the compression takes place inside the engine. When compared to the mixed compression engines the internal compression engines are a bit shorter.



a)



b)



c)

Figure 20: Different types of scramjet inlets a) External compression, b) External and internal compression and c) Internal compression

In the present project, the above-stated inlets have been attached to a regular scramjet engine model to obtain the characteristics of those inlets. The reference model is taken from the book 'Scramjet Propulsion' by E.T.Curran and S.N.B. Murty. The figure shows the reference model with dimensions.

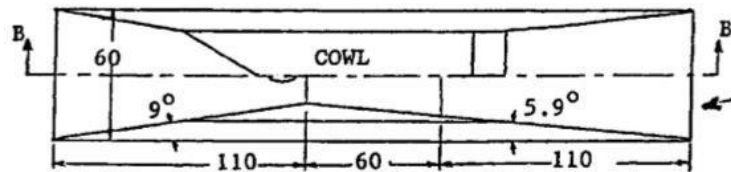


Figure 21: Scramjet engine reference model

1.2 Boundary conditions

The boundary conditions used for this simulation is the same as the first part of the project which are Dirichlet for inlet and Neumann for the outlet. Assumptions taken for the simulation are there is no slip at the walls and steady state computation is carried out.

1.3 Numerical Modelling

In any numerical modeling, flow governing equations affects the flow characteristics. For the present problem density-based solver is going to be used and assuming the flow is compressible and turbulent. The governing equations used for the project are Reynolds averaged Navier-Stoke (RANS) equations, which is useful to describe the position and characteristics of the shock wave and SST K- ω turbulence model.

Continuity equation

$$\frac{\partial \rho}{\partial t} + \frac{\partial(\rho u_i)}{\partial x_i} = 0 \quad \text{Where } i = 1,2,3$$

Momentum equation

$$\frac{\partial(\rho u_i)}{\partial t} + \frac{\partial(\rho u_i u_j)}{\partial x_i} + \frac{\partial P}{\partial x_i} = \frac{\partial(\rho \tau_{ij})}{\partial x_i} \quad \text{Where } i, j = 1,2,3$$

Energy equation

$$\frac{\partial(\rho e_t)}{\partial t} + \frac{\partial(\rho h_t u_j)}{\partial x_i} = \frac{\partial(\tau_{ij} u_i - q_i)}{\partial x_i} \quad \text{Where } i, j, t = 1,2,3$$

Species transport equation

$$\frac{\partial(\rho Y_i)}{\partial t} + \frac{\partial(\rho u_j Y_i)}{\partial x_j} = \frac{\partial(\rho u_i Y_i)}{\partial x_i} + \omega_i \quad \text{Where } i, j = 1,2,3$$

Turbulence modelling

$$\frac{\partial(\rho k u_i)}{\partial x_i} = \frac{\partial(\Gamma \frac{\partial k}{\partial x_j})}{\partial x_j} + G_k - Y_k + S_k \quad \text{Where } i, j = 1,2,3$$

$$\frac{\partial(\rho \omega u_i)}{\partial x_i} = \frac{\partial(\Gamma \frac{\partial \omega}{\partial x_j})}{\partial x_j} + G_\omega - Y_\omega + S_\omega \quad \text{where } i, j = 1,2,3$$

Where

ρ = Density

P = Pressure

h = Enthalpy

t = time

u = velocity component

τ_{ij} = Stress tensor

Y_i = Species mass fraction

ω_i = Chemical source term at a point i

q_i = Heat flux at a point i

Γ = Effective diffusivity

Y = Dissipation due to turbulence

D = Cross diffusion term

S = User defined sources

2. Results and Discussion

2.1 Results

The three types of inlets were tested in ANSYS to observe the flow characteristics. These results are going to be analyzed further to get clarity on using these inlets. The main characteristics involved in the performance of the scramjet engine are shock wave formation, shear layer formation and recirculation region. The analysis has been done at Mach numbers 6,8,10 and 12 to observe the behavior of shock waves at different mach numbers. The below are the pressure contour plots of external, mixed and internal inlet type engines.

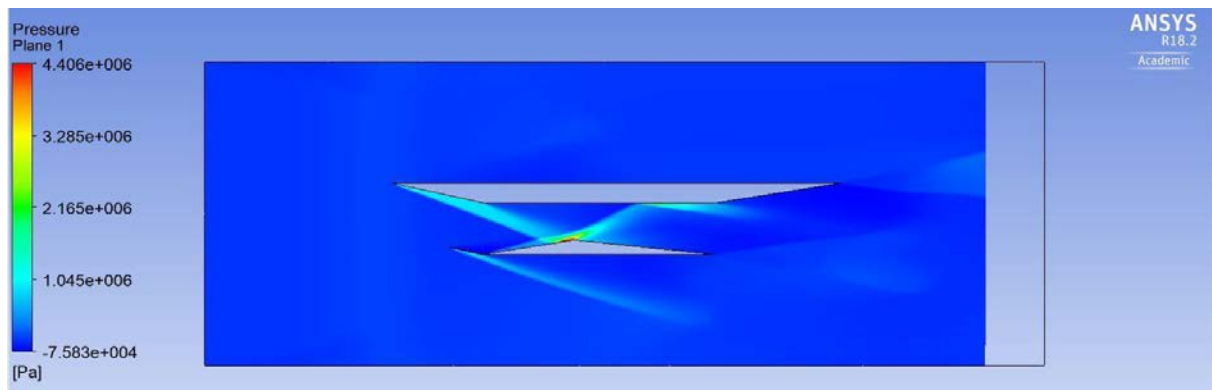


Figure 22: External inlet pressure contour at M=6

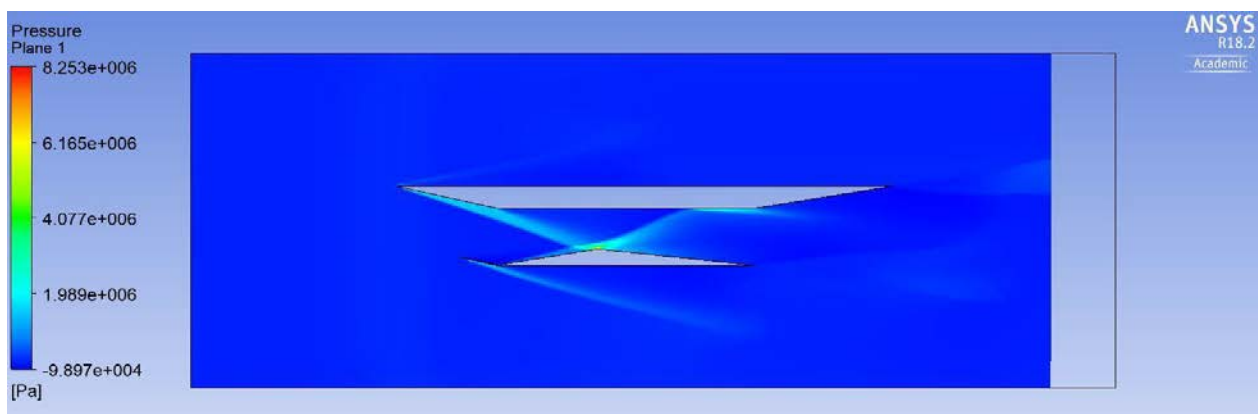


Figure 23: External inlet pressure contour at M=8

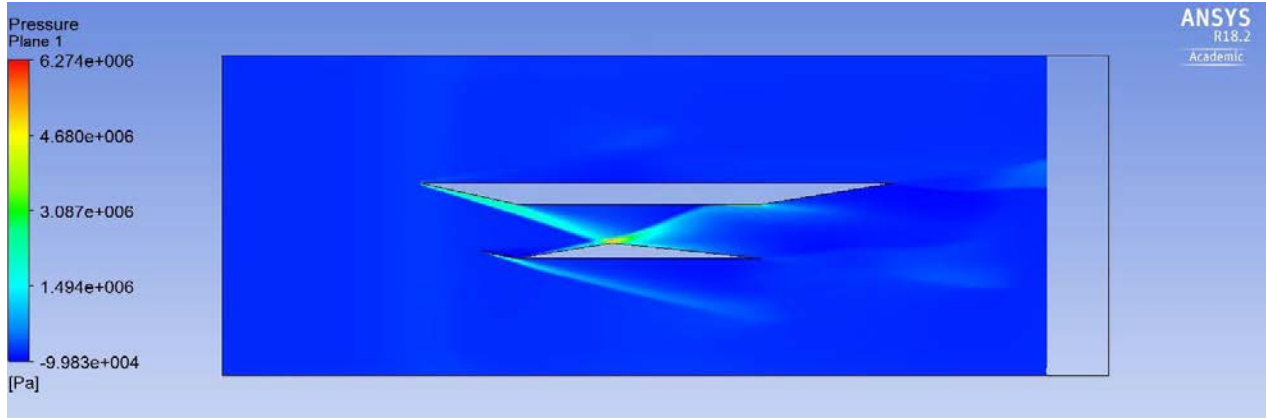


Figure 24: External inlet pressure contour at M=10

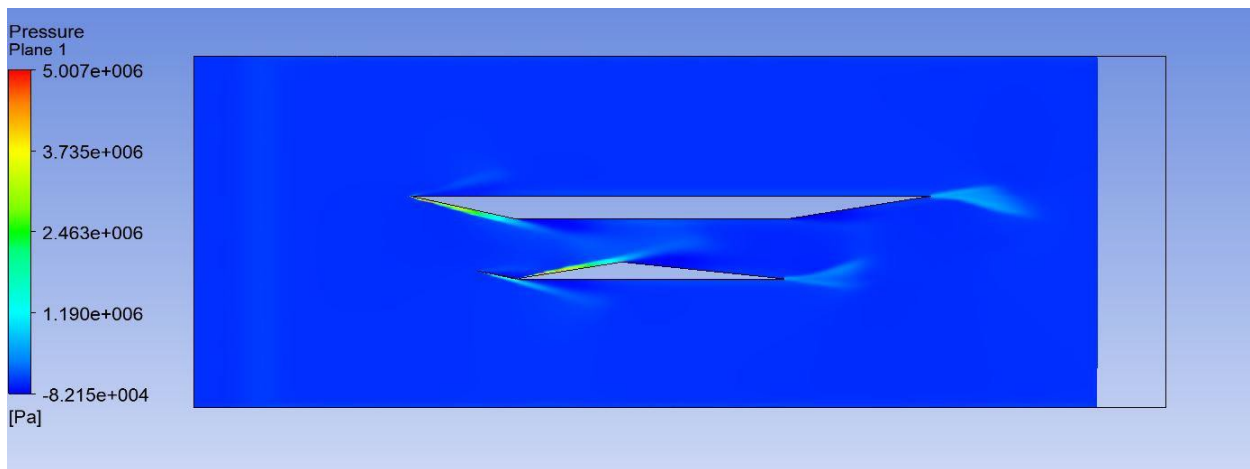


Figure 25: External inlet pressure contour at M=12

From the above figures, the compression takes place outside of the engine. As per the observation, the oblique shock waves were developed from the leading edge of the engine. When flow encounters the engine at mach numbers 6,8 and 10 the pressure is high at the end of the combustion chamber. But, in the case of mach 12 the pressure is throughout the combustion chamber. From the observation for this design, when the engine encounters mach 8 flow, it gave the highest-pressure values. So for this particular design mach 8 is preferable.

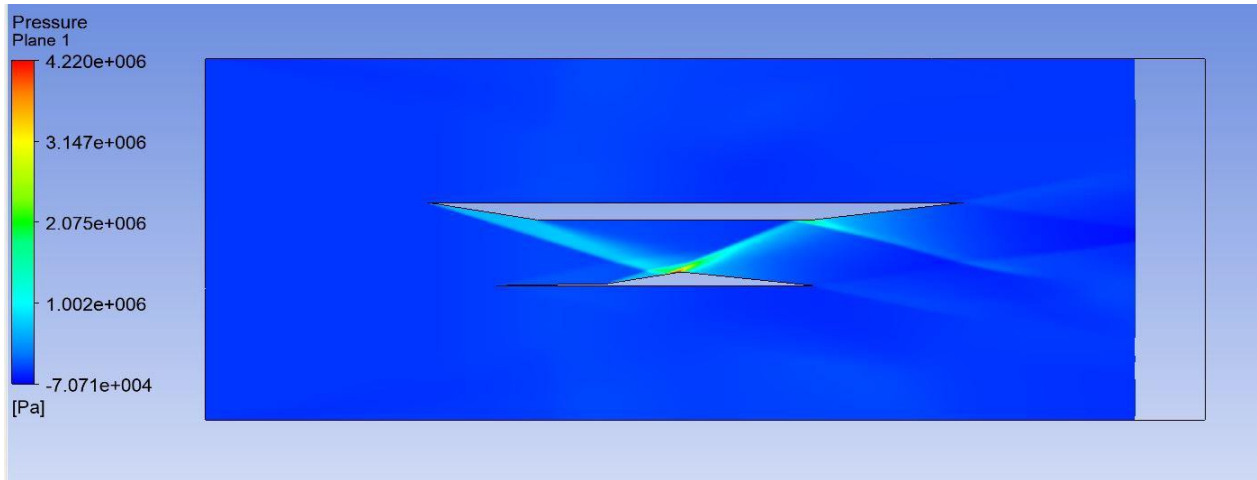


Figure 26: Internal and External inlet pressure contour at M=6

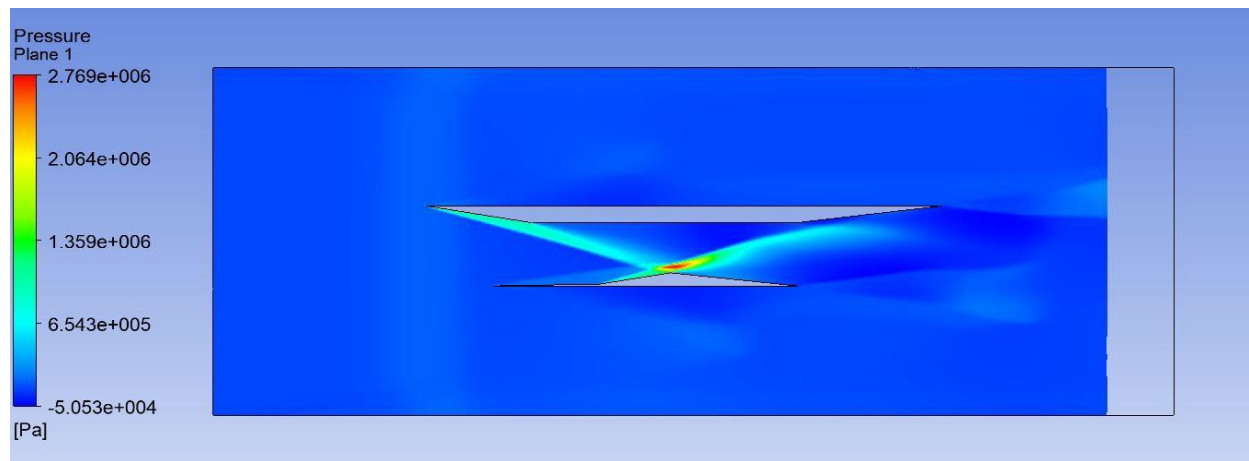


Figure 27: Internal and External inlet pressure contour at M=8

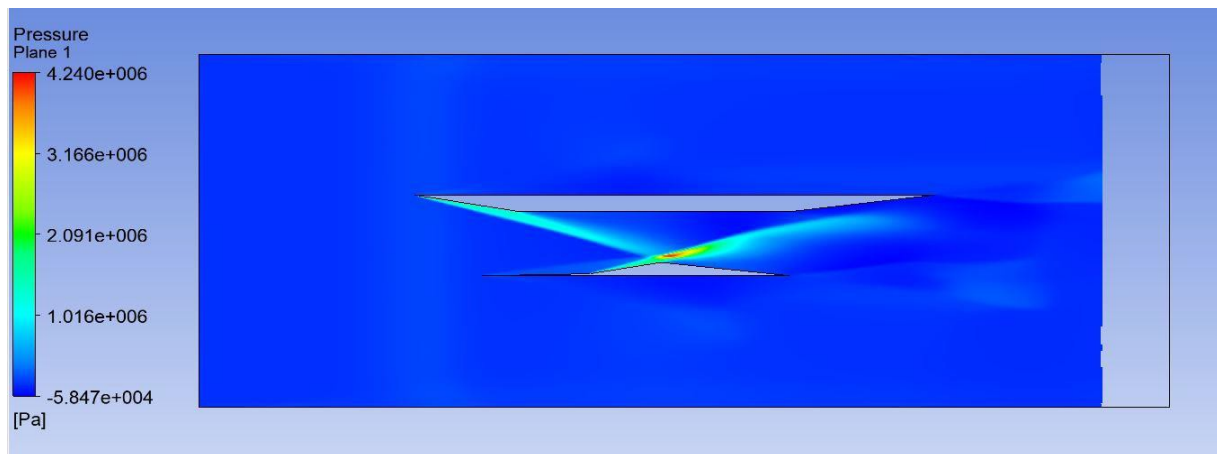


Figure 28: Internal and External inlet pressure contour at M=10

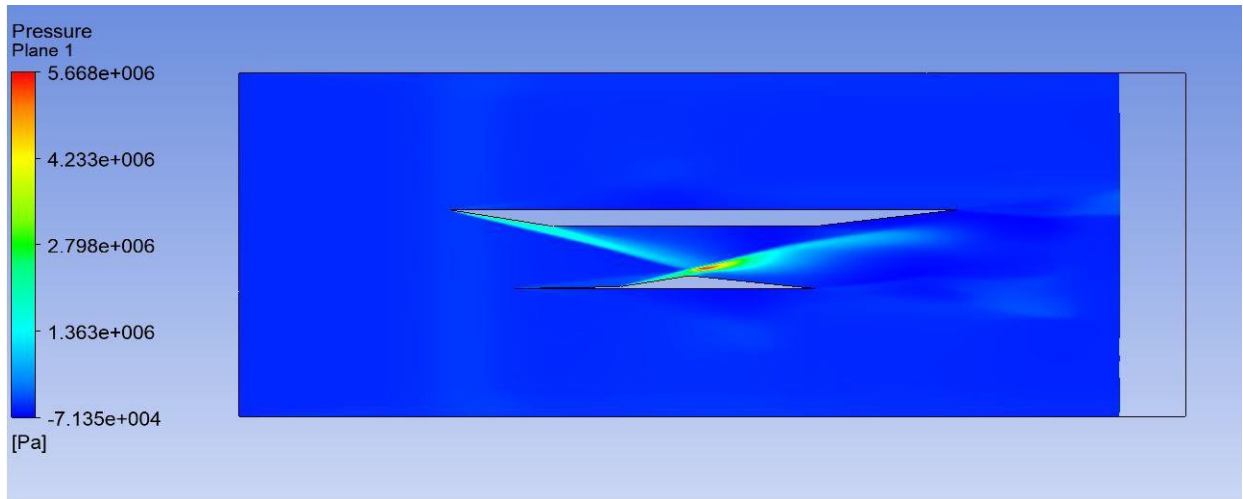


Figure 29: Internal and External inlet pressure contour at $M=12$

From observing the above internal and external pressure contour plots, the shockwaves were developed from the leading edge. Clearly, mixed compression takes place in this design. In this design, the high-pressure values were observed at the entrance of the nozzle which is not a good option for the combustion process. The mixed compression pressure values are very low when compared to the external compression inlet type.

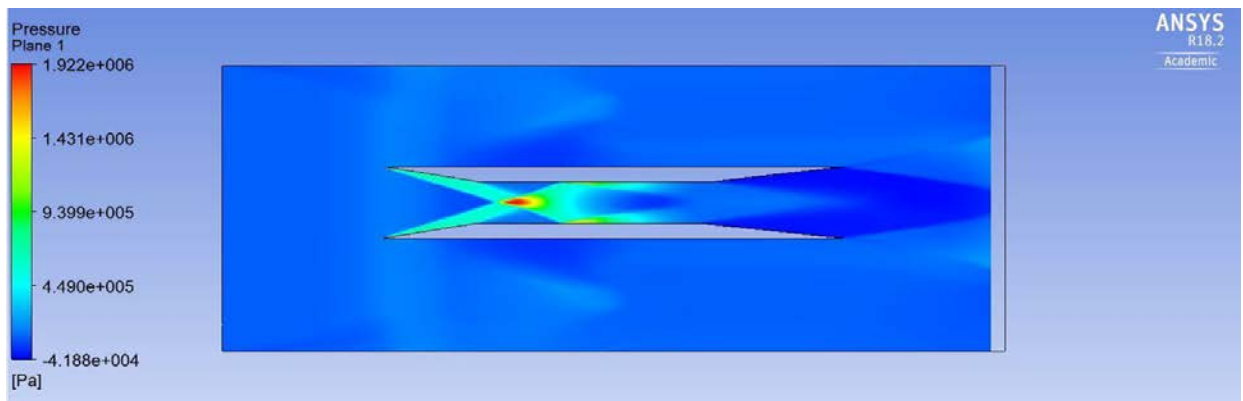


Figure 30: Internal inlet pressure contour at $M=6$

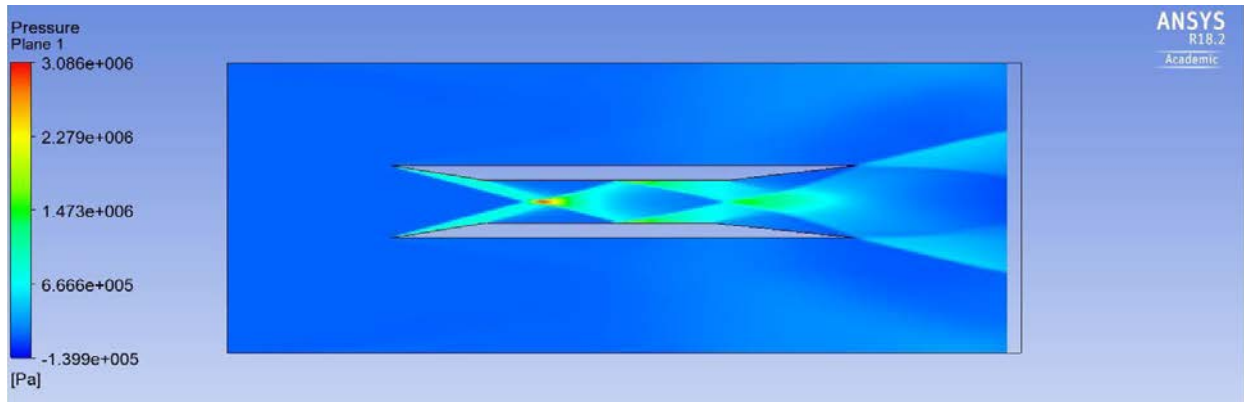


Figure 31: Internal inlet pressure contour at $M=8$

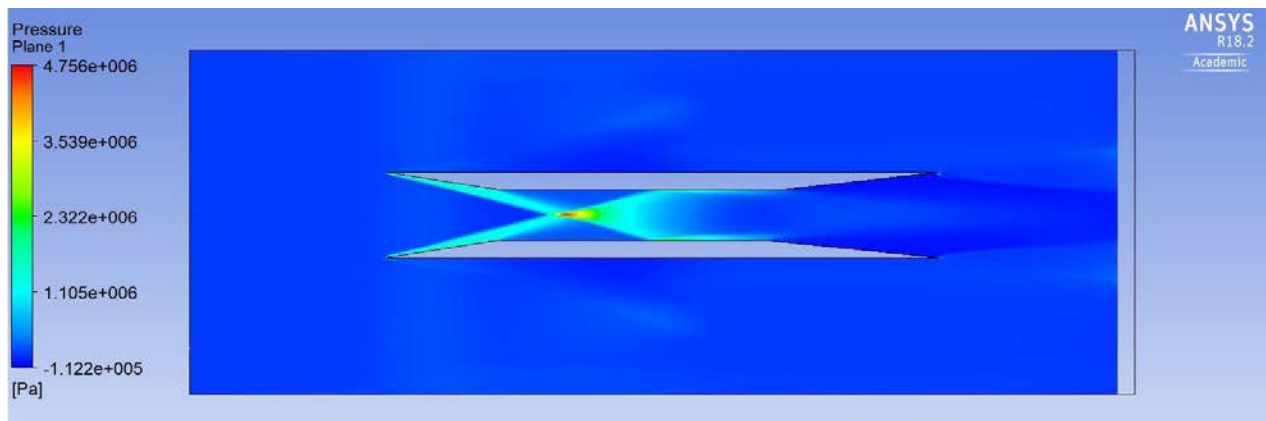


Figure 32: Internal inlet pressure contour at $M=10$

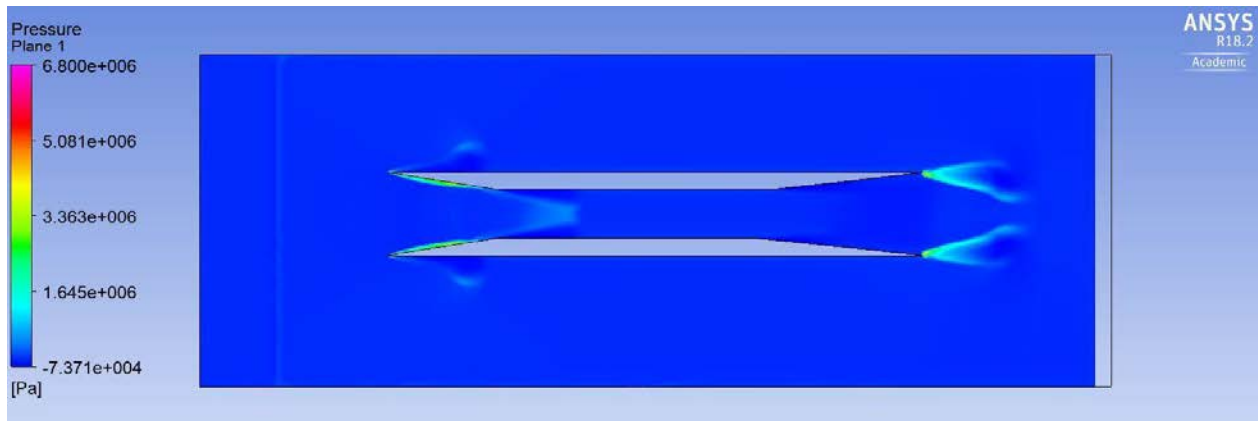


Figure 33: Internal inlet pressure contour at $M=12$

From the above contour plots, the compression takes place inside the engine. Here also, the shock waves were developed from the top and bottom walls of the inlet. The peak

pressure values were observed at the middle of the combustion chamber which is an advantage for the combustion process. In the case of external and mixed type inlets, the peak values were observed either at the end of the combustion chamber or at the inlet of the nozzle which is not more efficient for the combustion process.

2.2 Conclusion

The modelling and simulation of scramjet engine with three different inlets (external, mixed, internal) have been done in ANSYS-Fluent using RANS equations, SST k-omega model and finite rate eddy dissipation model. Since the scramjet engines don't carry compressors, there is a need of an efficient inlet. That means the inlet design should be very efficient to compress the high-speed air. So, in the present project, the three different inlet types were integrated with a regular scramjet engine model and simulation has been done at different Mach numbers (6,8,10 and 12). The trends have been observed through the pressure contour plots. As per the theory, if the pressure in the combustion chamber is high then there will be a chance of efficient combustion. From the external inlet type pressure contour plots, it was observed that pressure is high at the lower wall of the combustion chamber and the peak pressure was observed at the end of the combustion chamber. From the internal and external type combustion chamber pressure plots, the peak pressure values were observed at the entrance of nozzle which is not a favorable option for combustion. From the internal compression inlet type pressure plots, the pressure values were high throughout the combustion chamber and the peak pressure value was observed at the middle of the combustion chamber. So, from the observation internal compression type inlets giving better performance over the other two types.

References

1. Curran, E. T., & Murthy, S. N. (2000). *Scramjet propulsion*. Reston, VA: American Institute of Aeronautics and Astronautics.

Appendix

Velocity contours of external, mixed and internal compression types at different mach number.

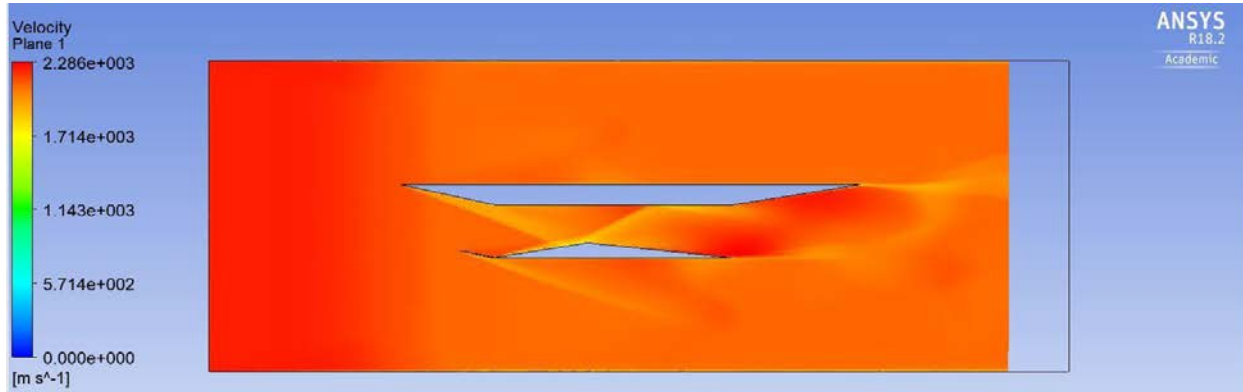


Figure 34: External inlet velocity contour at M=6

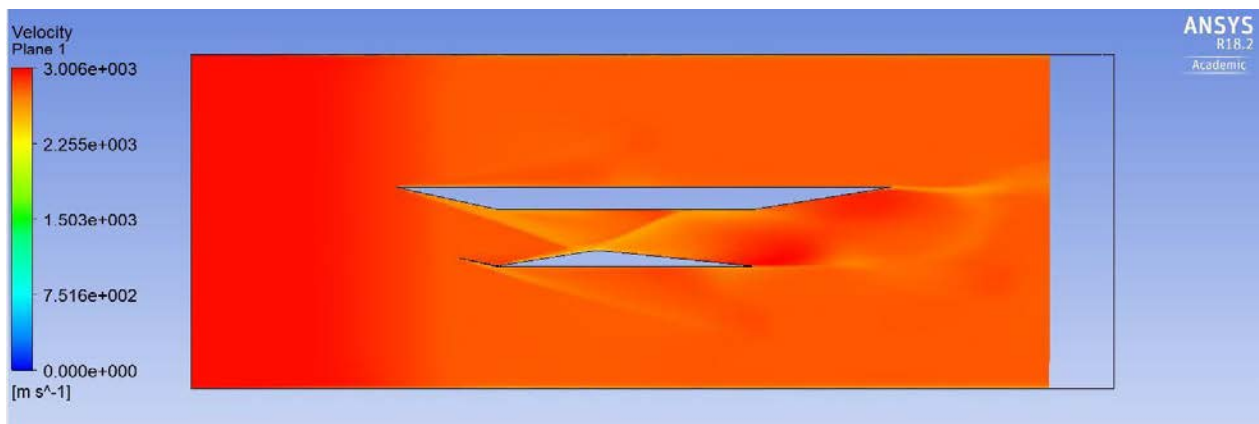


Figure 35: External inlet velocity contour at M=8

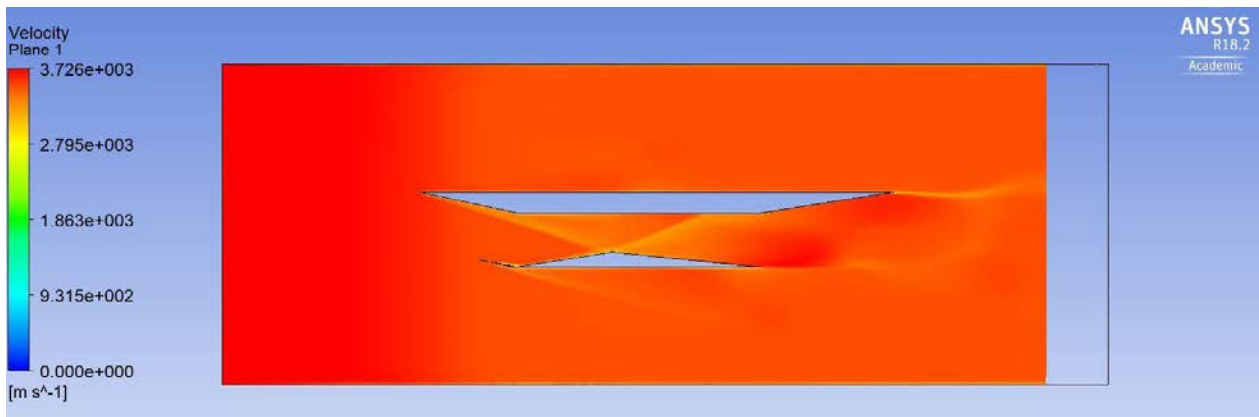


Figure 36: External inlet velocity contour at M=10

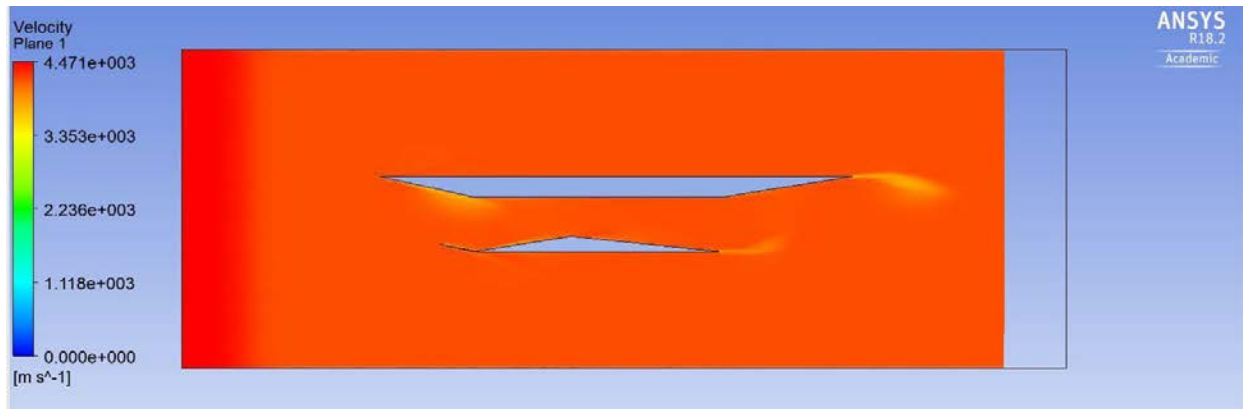


Figure 37: External inlet velocity contour at M=12

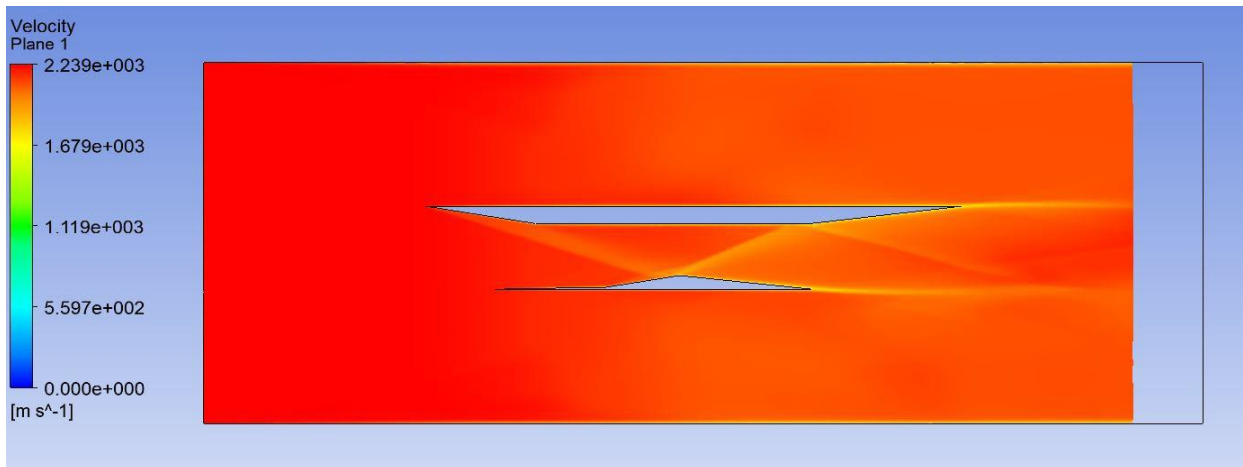


Figure 38: Internal and external inlet velocity contour at M=6

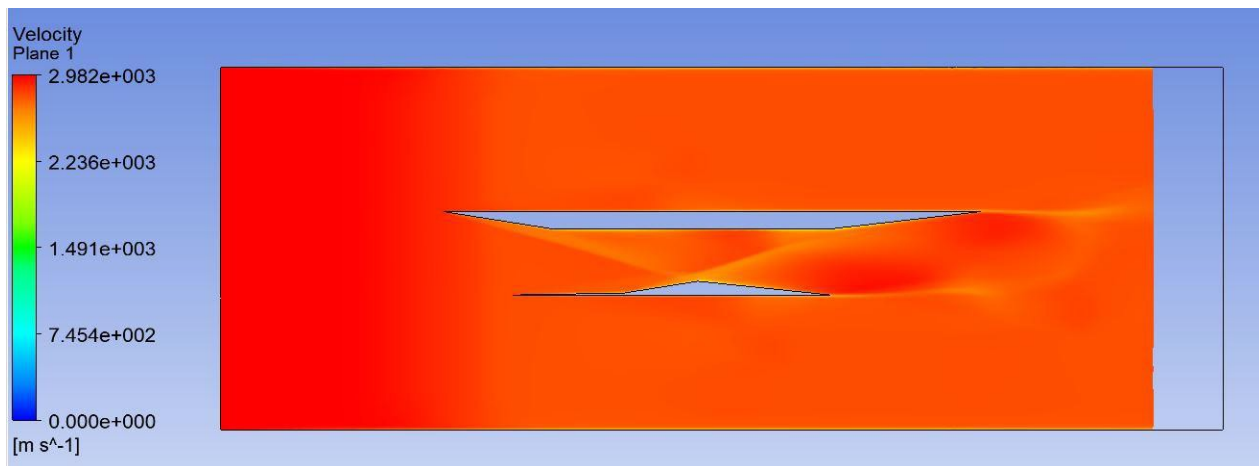


Figure 39: Internal and external inlet velocity contour at M=8

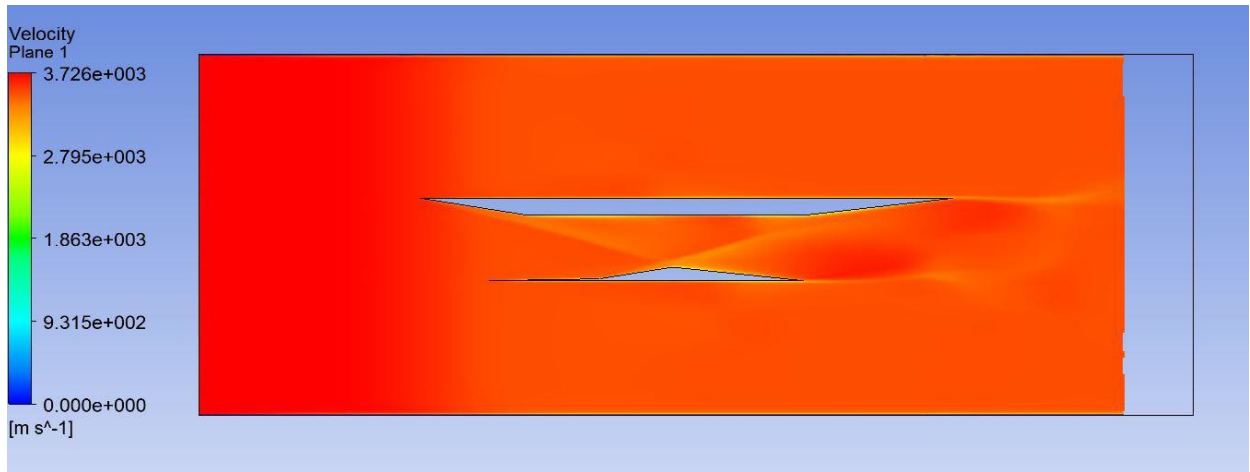


Figure 40: Internal and external inlet velocity contour at M=10

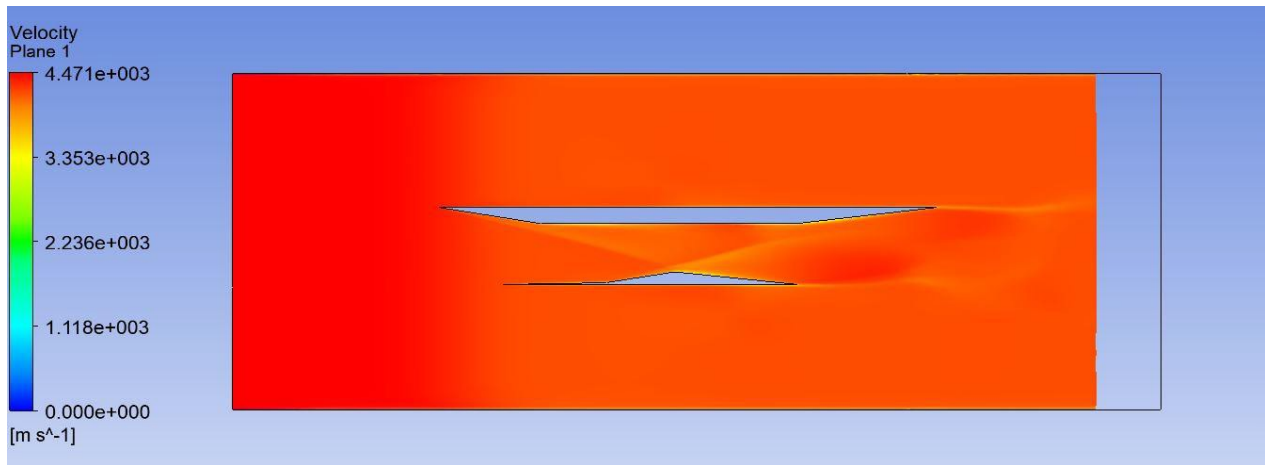


Figure 41: Internal and external inlet velocity contour at M=12

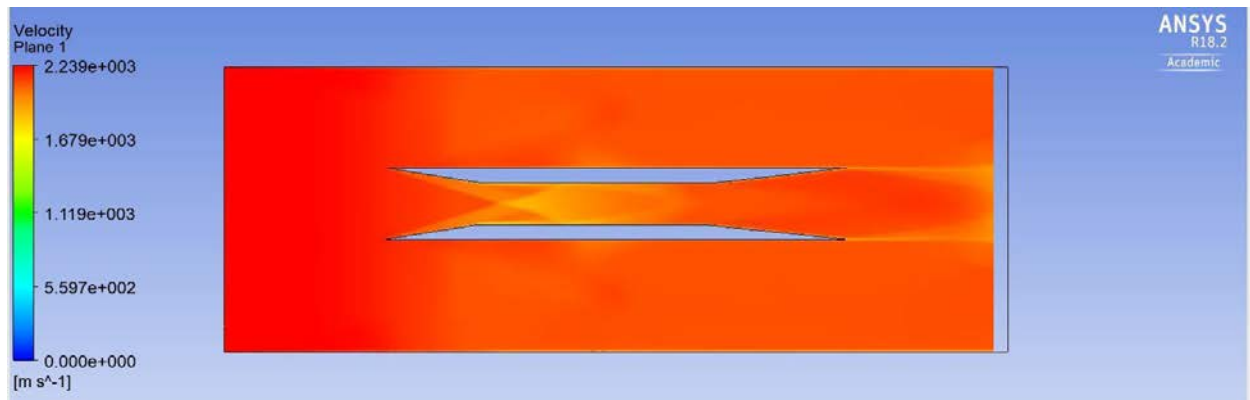


Figure 42: Internal inlet velocity contour at M=6

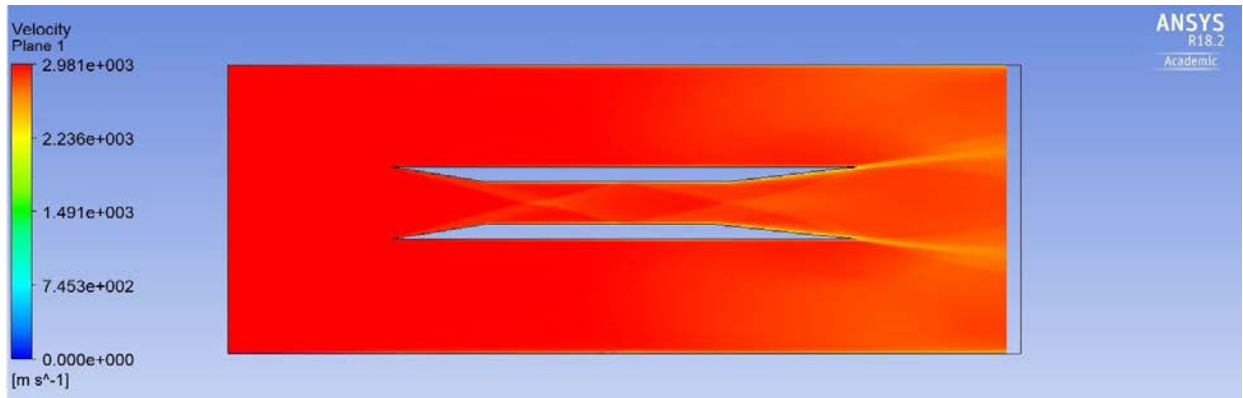


Figure 43: Internal inlet velocity contour at M=8

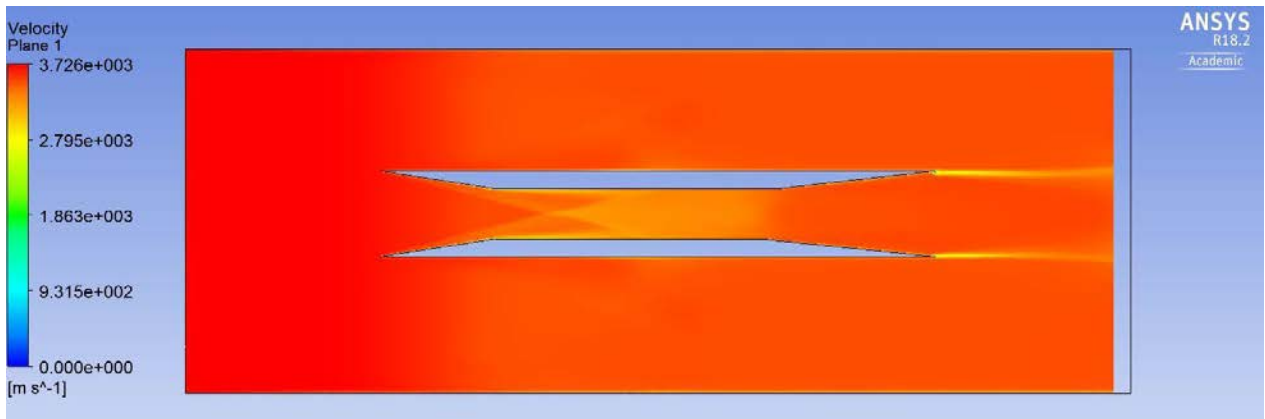


Figure 44: Internal inlet velocity contour at M=10

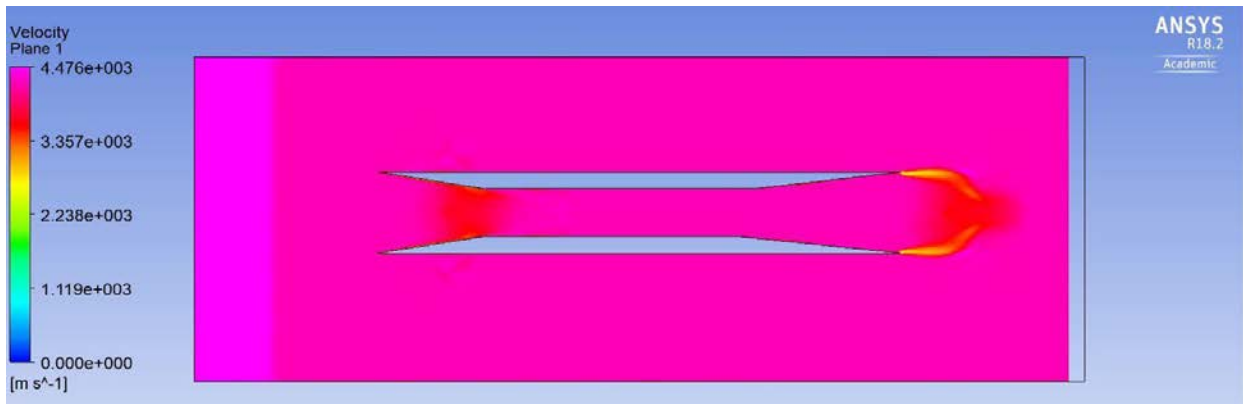


Figure 45: Internal inlet velocity contour at M=12

MATLAB code used for plotting Cross stream flow characteristics:

```
clc

clearvars

clear all

data=importdata('temp120.txt'); %% File to plot

length=data(:,1);

dlr=data(:,2);

spher_dlr=data(:,3);

step_dlr=data(:,4);

hold on

plot(dlr,length,'--*')

plot(step_dlr,length,'--*')

plot(spher_dlr,length,'--*')

xlabel('Temperature (K)'); %% Change the name

ylabel('Length (m)'); %% Change the name

title('Cross Stream Temperature at x=120 mm');

legend on

legend('Standard DLR','Step DLR','Spherical DLR')
```